Fumarate production with *Rhizopus oryzae*: utilising the Crabtree effect to minimise ethanol by-product formation

Reuben Marc Swart

December 2019

Fumarate production with *Rhizopus oryzae*: utilising the Crabtree effect to minimise ethanol by-product formation

Reuben Marc Swart

A dissertation submitted in partial fulfilment of the requirements for the degree

Master of Engineering

in the

Department of Chemical Engineering
University of Pretoria

Supervisor: Prof. Willie Nicol

December 2019

Fumarate production with *Rhizopus oryzae*: utilising the Crabtree effect to minimise ethanol by-product formation

Synopsis

Fumarate has been identified as a promising biomass-derived chemical building block. Fumarate is a dicarboxylic acid that forms part of the tricarboxylic acid cycle. The double carbon bond in fumarate positions it as a versatile chemical capable of multiple applications. Conversion of fumarate to maleic anhydride is particularly interesting since maleic anhydride has a large market and is currently petrochemically produced. *Rhizopus oryzae* has been found to be the most promising organism for producing fumarate. The production of fumarate is induced by nitrogen-limited conditions, and this production has always been associated with the unwanted parallel excretion of ethanol. Efforts to negate the production of ethanol have focused on oxygen availability. The literature states that anaerobic zones within the mycelium matrix are responsible for the production of ethanol. The Crabtree effect is a phenomenon first discovered in *Saccharomyces cerevisiae* fermentations. It is described as the production of ethanol in an aerobic environment. In this study, we intended to test whether a strategy of controlled glucose addition can negate the production of ethanol during biomass growth and fumarate production.

All fermentations were performed with either nitrogen excess (growth phase) or nitrogen limitation (production phase), with medium replacements being done between the growth phase and the production phase. To test whether the production of ethanol is linked to the availability of oxygen, two production fermentations were conducted at different dissolved oxygen values (18.4 % and 85 %). Similar ethanol production rates were observed at both these dissolved oxygen values, indicating that there is no relation between oxygen and ethanol production for the specific morphology. This suggests that ethanol is produced as an overflow product as part of the Crabtree effect. *S. cerevisiae* biomass is grown using a controlled glucose addition to limit ethanol production. A similar strategy used in an *R. oryzae* production fermentation revealed that it was possible to produce biomass without the production of ethanol. A similar strategy was utilised in a fumaric acid production fermentation to test whether ethanol production can be removed. It was found that a glucose feed rate of $0.197\,\mathrm{g\,L^{-1}\,h^{-1}}$ produced $0.15\,\mathrm{g\,L^{-1}\,h^{-1}}$ of fumarate while not producing ethanol. It was further discovered that ethanol overflow commences at a glucose addition rate of $0.395\,\mathrm{g\,g^{-1}\,h^{-1}}$ on biomass, while the threshold glucose uptake

rate was established to be between $0.426\,\mathrm{g\,g^{-1}\,h^{-1}}$ and $0.533\,\mathrm{g\,g^{-1}\,h^{-1}}$.

It has been conclusively proved that *R. oryzae* is a Crabtree-positive organism and that this phenomenon can be utilised to negate the production of ethanol during growth and production fermentations. The term homofumarate production" is used to describe the condition where all carbon exits the cell as either fumarate or respiratory CO_2. The result provides new insights toward developing a high-yield industrial process to produce fumaric acid with *R. oryzae*.

Further exploratory work was done on the effect of the urea feed rate. It was found that a higher urea addition rate shifted both the ethanol overflow point and the glucose threshold glucose uptake rate. A more in-depth investigation needs to be conducted to uncover the mechanism involved.

Acknowledgements

- I thank God, Jesus Christ for giving me the ability to glorify His name through this research and for providing for me at every turn.
- Prof. Willie Nicol, thank you for educational guidance and financial support through this research. You have become a friend.
- The financial support of the National Research Foundation (NRF) is greatly appreciated. Opinions expressed are those of the author and not necessarily attributed to the NRF.
- Nico de Jongh, Sekgetho Mokwatlo, Naas van Rooyen and Eleanor Smit, thank you for making the long hours spent in the lab enjoyable.

Dedication

I dedicate this work to my parents, Marc and Self Swart, I thank you for the constant support and love.

Contents

List of Figures

Nomenclature

α	Carbon dioxide yield coefficient	$Cmol\ CO_2\ Cmol\ X^{-1}$
β	NADH yield coefficient	$mol\ NADH\ Cmol\ X^{-1}$
γ	ATP yield coefficient	$mol\ ATP\ Cmol\ X^{-1}$
μ_{max}	Maximum specific growth rate	h^{-1}
C_i^o	Concentration of species i in the feed	$g\ L^{-1}$ or $mol\ L^{-1}$
C_i	Concentration of species i in the reactor	$g\ L^{-1}$ or $mol\ L^{-1}$
C_x	Concentration of biomass in the reactor	$g\ L^{-1}$
K_m	Monod constant	$g\ L^{-1}$
N_i	Mass of species i	g
Q	Exit flow rate	$L\ h^{-1}$
Q_o	Intel flow rate	$L\ h^{-1}$
Q_{gas}	Gas flow rate	L
r_i	Rate of production of species i	$g\ g^{-1}\ h^{-1}$
r_x	Rate of biomass growth	$g\ g^{-1}\ h^{-1}$
r_{CO2}	Rate of CO_2 production	$mol\ L^{-1}\ h^{-1}$
t	Time	h
V	Reactor volume	L
V_g	Gas volume of reactor	L
Y_{Si}	Yield coefficient of species i on glucose	$mol\ i\ Cmol\ S^{-1}$

List of abbreviations

α-KET	alpha-Ketoglutarate
ACE	Acetaldehyde
ASL	Argininosuccinate lyase
ATP	Adenosine triphosphate
CIT	Citrate
DHAP	Dihydroxyacetone phosphate
ETC	Electron transport chain
$FADH_2$	Flavin adenine dinucleotide
FUM	Fumarate
GTP	Guanosine-5-triphosphate
HPLC	High performance liquid chromatography
MAL	Malate
MDH	L-malate dehydrogenase
NADH	Nicotinamide adenine dinucleotide
OXA	Oxaloacetate
PDA	Potato dextrose agar
PYC	Pyruvate carboxylase
PYD	Pyruvate decarboxylase
SUC	Succinate
TCA	Tricarboxylic acid cycle

1 Introduction

Global factors such as the drive to decrease carbon emissions and the interest in more green chemistry has increased the demand for biologically produced chemicals. Fumaric acid has been named one of the top ten biomass-derived chemical building blocks (Werpy & Petersen, 2004). Fumaric acid (FA) is a versatile compound and therefore has a wide variety of applications. It has been used in resins, polyesters, animal feeds, medical treatments and the food and beverage industries. Fumaric acid is currently produced from maleic anhydride (Roa Engel, Straathof, *et al*, 2008). The production of maleic anhydride uses benzene or butane as a feed-stock which is then oxidised with a vanadiumphosphorus oxide catalyst. This reaction is very exothermic, producing large amounts of CO and CO_2, resulting in typical yields of maleic anhydride from butane of 75 % (Felthouse *et al*, 2001; Wojcieszak *et al*, 2015).

The production of fumaric acid through biological routes, such as the use of *Rhizopus oryzae*, has received more attention lately in an effort to move away from our reliance on fossil fuels. The use of organisms to produce chemical compounds is particularly appealing since renewable forms of biomass can be used as the feed-stock. Fumaric acid is an essential part of the tricarboxylic acid cycle, which is a vital part of the respiratory mechanism of all eukaryotes. Fumaric acid is produced naturally by the plant *Fumaria officinalis*, the mushroom *Boletus fomentarius* and by human skin when it is exposed to sunlight (Committee of Experts on Cosmetic Products, 2008). However, the preferred organism for the production of fumaric acid is *R. oryzae* (Sebastian *et al*, 2019).

R. oryzae is a filamentous fungus that excretes fumarate as a response to nitrogen-limited environmental conditions (Ilica *et al*, 2019). There are two groups of *R. oryzae* namely, lactic acid producers and fumaric-malic acid producers. The latter is more correctly named *Rhizopus delemar*, but the literature still refers to it as *R. oryzae* (Abe *et al*, 2007). *R. oryzae* ATCC 20344 is one of the most studied strains in the *Rhizopus* genus. Numerous genetic modifications have been made to this strain to improve the production of fumarate, but only minor improvements have been seen (Deng *et al*, 2012; Kang *et al*, 2010). The modified strains were not able to produce titres comparable to those of the wild strains or did not pass on the traits to the following generations. Titres in the range of $25\,\mathrm{g\,L^{-1}}$ to $103\,\mathrm{g\,L^{-1}}$ and volume-based productivities ranging from $0.19\,\mathrm{g\,L^{-1}\,h^{-1}}$ to $1.21\,\mathrm{g\,L^{-1}\,h^{-1}}$ are commonly obtained by the wild strains of *R. oryzae* (Sebastian *et al*, 2019).

To move away from the petrochemical-reliant production of fumarate, lignocellulosic biomass is seen as a promising replacement for crude oil. Biomass is renewable and can be sustainably produced. Glucose is the substrate most commonly used for studying

the production of fumarate. This is because glucose is a monomer unit that forms part of many polysaccharides, which are compounds widely found in all biomass and will be easily obtainable for an industrial process. The use of glucose also simplifies the metabolic flux analysis since the substrate can be clearly defined, unlike a complex substrate such as corn stover.

Production of fumarate with *R. oryzae* is induced by limiting the nitrogen content in the medium and providing excess glucose. Fumarate production has always been associated with the co-excretion of ethanol. The production of ethanol is unwanted since it is a waste of carbon and therefore decreases the yield of fumarate on glucose. Downstream separation can also be negatively affected by the presence of ethanol. Numerous authors have attributed the production of ethanol to anaerobic zones forming in the mycelium matrix (Y Zhou, Du & Tsao, 2000; Suijdam, Kossen & Paul, 1980; Liao *et al*, 2007). The proposed method of negating ethanol production is by reducing the diameter of suspended *R. oryzae* pellets. Although this is the proposed method no study has conclusively shown this to reduce ethanol formation.

In this study it is postulated that the production of ethanol in *R. oryzae* fermentations is a result of carbon overflow caused by the Crabtree effect. The Crabtree effect was first discovered in *Saccharomyces cerevisiae* and is defined as the production of ethanol as a result of limited respiratory capacity in a fully aerobic environment (Barford & Hall, 1979). *S. cerevisiae* is a facultative anaerobe, as is *R. oryzae*. Facultative anaerobes can produce ATP through respiration when oxygen is present and under anaerobic conditions where fermentative pathways are used to produce ATP (Habegger, Crespo & Dabros, 2018). *S. cerevisiae* is one of the most widely studied microorganisms, and the findings from these studies can often be applied to other organisms when similar traits are shared. Ethanol is produced as a response to an oversupply of glucose since respiration is not able to accommodate the rate of glucose uptake. To produce *S. cerevisiae* biomass Habegger *et al* (2018) used a glucose-control strategy to limit ethanol production while increasing the yield of biomass. It is proposed that using a similar approach could be effective in negating the co-excretion of ethanol in *R. oryzae* fumarate production fermentations.

In this study, it will first be definitively determined whether *R. oryzae* produces ethanol as a result of anaerobic zones in the mycelium matrix or as a result of it being a Crabtree-positive organism. Fermentations will be conducted in which the dissolved oxygen values in the medium will be varied while the production of ethanol is monitored. In the following experiments, a controlled glucose addition strategy will be employed to negate ethanol production in the biomass production phase and the fumarate production phase. Fungal biomass is conventionally grown with excess glucose and nitrogen as shown in the first scenario of Figure 1a. Here glucose uptake is controlled by the organism and the energy

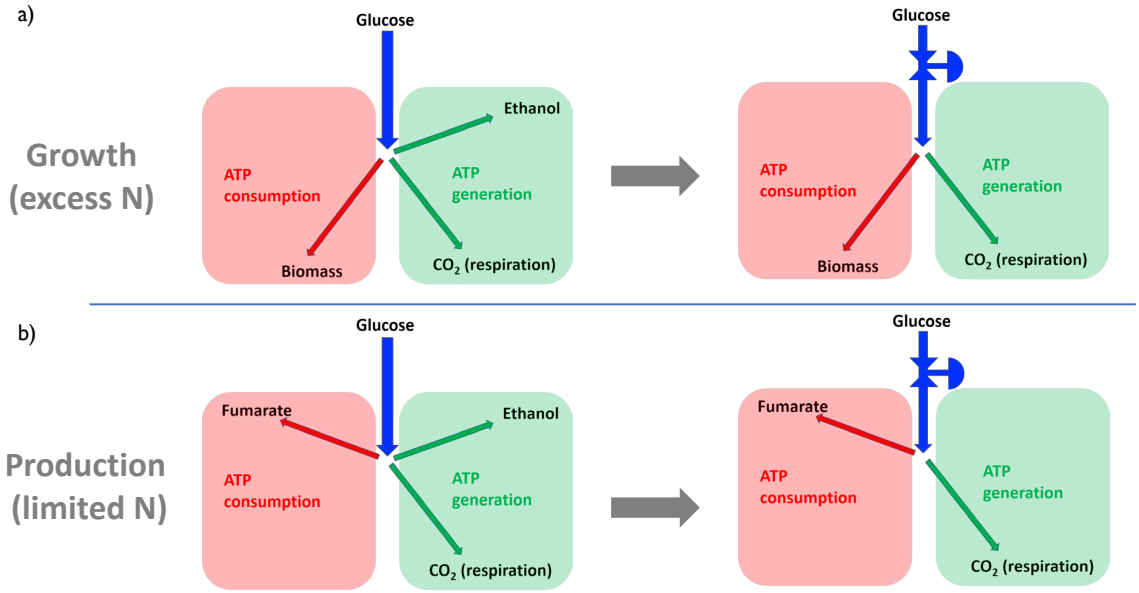

Figure 1: The postulated effect of glucose limitation on growth and fumarate production fermentations. Glucose uptake rates are controlled via fed-batch fermentation and are indicated with a reducing valve on the incoming glucose flux. It is postulated that glucose throttling will reduce ethanol formation in both growth and fumarate production fermentations.

demand for biomass production is supplied by respiration and the production of ethanol. The second scenario of Figure 1a proposes a controlled glucose addition to negate the production of ethanol. The excretion of fumarate also consumes energy (ATP) as a result of the acid transport costs from the cell into the medium (Taymaz-Nikerel *et al*, 2013). Based on the hypothesis, ethanol is produced as a result of a glucose uptake rate that exceeds the respiratory capacity of the cell. Ethanol is therefore excreted to avoid accumulation within the cell. This is hypothesised to be true for ethanol production during biomass growth and fumarate production. Figure 1b illustrates the proposed effect of controlling the glucose addition rate during fumarate production. Naude & Nicol (2018) have developed an immobilised biomass bioreactor system to produce fumarate from glucose with *R. oryzae*. This system will be adapted for all the experiments in this study.

2 Literature review

2.1 Fumaric acid

Fumaric acid, also known as (E)-Butenedioic acid, is an organic molecule that forms a vital part of the tricarboxylic acid cycle. Fumaric acid received its name from the plant, *Fumaria officinalis*, in which it was first discovered. The structure and functional groups of fumaric acid make it a versatile chemical. It has two terminal carboxylic acid groups and a double carbon bond in the α, β position as shown in Figure 2 (Das, Brar & Verma, 2016). This structure positions fumaric acid between maleic acid and succinic acid since fumaric acid can easily be isomerised to maleic acid or hydrogenated to succinic acid (Wojcieszak *et al*, 2015). Heat treatment can also be used to form maleic anhydride which has a 2.1 $\mathrm{Mt\,a^{-1}}$ market (Grand View Research, 2014).

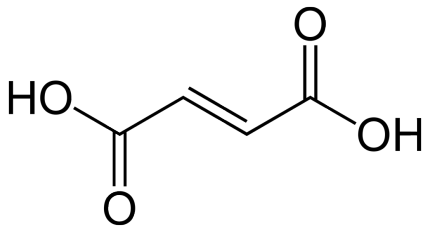

Figure 2: Fumaric acid structure

Fumaric acid has a far lower solubility than malic acid which has a more polar structure as a result of the cis carboxylic groups (*The Oxford Encyclopedia of Food and Drink in America* 2012). Although the solubility of malic acid is favoured in food and beverage applications, the separation of fumaric acid is easier as a result of the lower solubility (Giorno *et al*, 2001; Felthouse *et al*, 2001; Roa Engel, Gulik, *et al*, 2011). During the microbial production of carboxylic acids the low solubility of fumaric acid is favoured. Low pH values impact the solubility of fumaric acid causing it to precipitate. This does not occur with other acids and, therefore, at low pH values the extracellular concentration is lower for fumaric acid than for other acids (Taymaz-Nikerel *et al*, 2013). This reduces the ATP costs of transporting the acid from the cell into the medium and should result in a higher yield of fumaric acid since less energy was used to export it into the medium.

2.2 Fumaric acid market and applications

2.2.1 Economy of four-carbon dicarboxylic acids

The four-carbon dicarboxylic acids of the TCA cycle have been identified as top value-added chemicals from biomass (Werpy & Petersen, 2004; Bozell & Petersen, 2010). The goal of these reports was to promote biomass-derived chemicals that will drive the biorefinery economy. Key factors were found to be improving the use of feed stocks, waste streams, by-products, equipment, and shared practices to bring down the production costs by improving productivity and efficiencies. These reports have been used as motivation for numerous studies of the production of fumaric acid and this has led to improvements in production(Taymaz-Nikerel *et al*, 2013; Naude & Nicol, 2018; Roa Engel, Straathof, *et al*, 2008; Z Zhou *et al*, 2011; G Wang *et al*, 2013; Sebastian *et al*, 2019). Many studies have focused on the biological production of succinic acid and this has led four industrial startups to use biological routes to produce succinic acid (Jansen & Gulik, 2014). However, no industrial bioprocess has yet been established to produce fumaric acid (Das, Brar & Verma, 2016). Roa Engel, Straathof, *et al* (2008) state that the production of fumaric acid with *R. oryzae* is still not economically comparable to the petrochemical synthesis. This statement is, however, heavily based on the raw material costs which may no longer apply with the increasing cost of fossil fuels.

Currently, fumaric acid is produced by the isomerisation of maleic acid which is produced by hydrolysing maleic anhydride. All maleic anhydride is produced by catalytic reaction of butane. Figure 3 illustrates the chemical synthesis to convert butane into fumaric acid. This reaction uses vanadyl pyrophosphate, $(VO)_2P_2O_7$, as the catalyst and is the only commercial economically viable route to produce maleic anhydride from butane (Das, Brar & Verma, 2016). The oxidation of butane to maleic anhydride is very exothermic and produces CO and CO_2 as the main by-products. More than 225 US patents have been published on this synthesis since 1980 (Felthouse *et al*, 2001). This intensive research has brought down the cost of petrochemically producing maleic anhydride and fumaric acid. A capital investment this large may be an influencing factor explaining why the industry is slow to change. The global fumaric acid market is estimated to be $322\,000\,\mathrm{t\,a^{-1}}$ and this is projected to grow to $385\,000\,\mathrm{t\,a^{-1}}$ in 2022 (Grand View Research, 2019). All fumaric acid produced from maleic anhydride accounts for 3 % of the total maleic anhydride market (Roa Engel, Straathof, *et al*, 2008).

2.2.2 Current and future applications

Fumaric acid is the protonated form of fumarate. As a result of fumaric acid having a double carbon bond and two terminal carboxylic groups, it is a versatile chemical and is known as a chemical building block (Werpy & Petersen, 2004). Building blocks are defined as chemicals that possess useful functional groups that can be transformed into new, more valuable chemicals. Figure 3 illustrates some of the more common chemicals into which fumaric acid can be transformed. Fumaric acid is an isomer of maleic acid, the difference between the compounds being the trans and cis orientation around the double carbon bond. Although fumaric acid is a very valuable chemical is it not as widely produced or consumed as maleic anhydride. Maleic anhydride produced from petrochemical feed stocks has a 2.1 Mt a^{-1} market (Grand View Research, 2014). Simple conversion of fumaric acid to maleic anhydride is an attractive property, especially if fumaric acid can be produced inexpensively through fermentation pathways. It has been found that a 96 % yield of maleic anhydride can be achieved from fumaric acid (Nystrom, Loo & Leak, 1952). The dehydration reaction uses phosphorus pentoxide as a catalyst at temperatures between 155 °C and 160 °C. The product can then be collected via a condensation trap and air-dried to produce the final product.

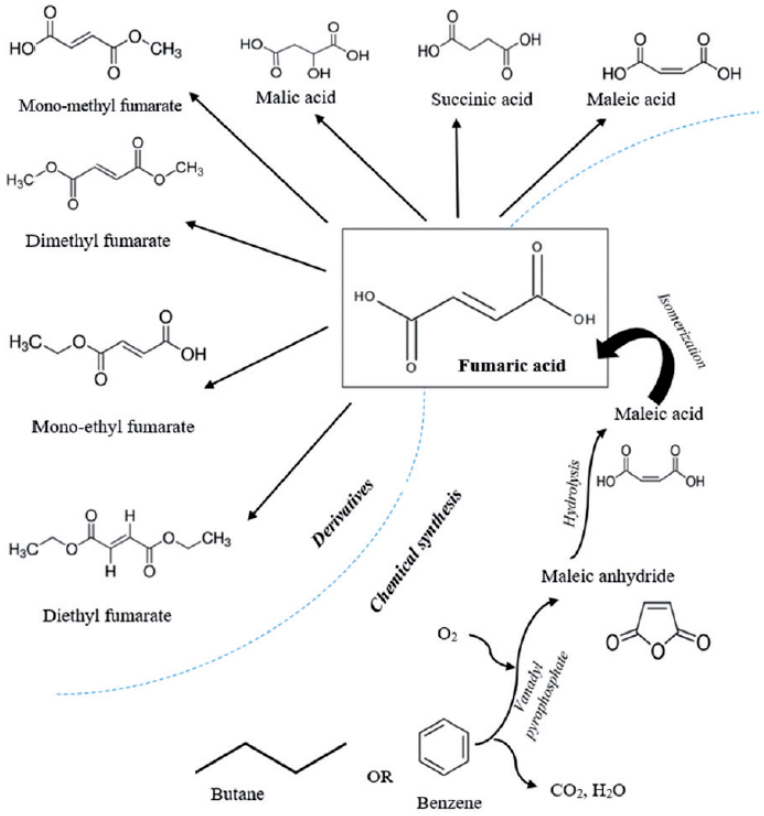

Figure 3: Fumaric acid petrochemical synthesis and it's derivatives (Sebastian *et al*, 2019)

Fumaric acid has relatively low solubility in water compared with malic acid, and for this

reason malic acid is the favoured acidulant in food and beverage applications (Giorno *et al*, 2001; Felthouse *et al*, 2001). It has been found that it is possible to hydrate fumaric acid to malic acid through bio-conversion with *R. oryzae* or *S. cerevisiae* (Naude & Nicol, 2018; Stojkovič & Žnidaršič-Plazl, 2012). Current market estimates state that 33 % of fumaric acid is used by the food and beverage industry and this sector is expected to increase as a result of its use in energy drinks and energy bars (Grand View Research, 2019). Applications include pH control since it has more buffering capacity than other acids, gives better control of microbial growth and can be used as a flavour enhancer since it has a long-lasting sourness and flavour (Das, Brar & Verma, 2016). The non-toxic nature of fermentation-derived fumaric acid is favoured over fumaric acid produced chemically since the letter carries a toxicity risk.

It has been found that fumaric acid as an animal feed additive fumaric acid has the ability to reduce the production of methane from livestock by 32 % and improve the feeding efficiency (Z Li *et al*, 2018; Das, Brar & Verma, 2016). This has particular relevance considering the necessity to curb greenhouse gas emissions and the fact that livestock account for 12 % to 17 % of global methane emissions (Lassey, 2008). The emission of methane into the atmosphere has been found to contribute to global warming and is more harmful than CO_2.

It has been found that fumaric acid esters are an effective treatment for psoriasis. The treatment is not a new discovery, but was a licensed treatment only in Germany until recent approval was granted for the use of dimethylfumarate in the European Union (Warren *et al*, 2019). Fumaric acid esters have also been found to be immunomodulatory, which means that they can affect the body's immune system. Moharregh-Khiabani *et al* (2009) found this to be an effective treatment for multiple sclerosis and further studies are now investigating the long-term effects of fumaric acid ester treatment.

2.3 Microbial production of fumaric acid

The *Rhizopus* genus is by far the most popular organism used for the production of fumaric acid. This is clearly illustrated in the review papers published by Sebastian *et al* (2019) and by Ilica *et al* (2019). Pfizer the American pharmaceutical company, used *Rhizopus oryzae* in the 1940s to produce about 4000 t a^{-1} of fumaric acid. This continued until chemical synthesis became a more lucrative option (K Zhang, B Zhang & Yang, 2013). Foster & Waksman (1939) conducted a study in which 41 cultures were surveyed for fumaric acid production. They found that 9 of these cultures excreted fumaric acid. The genera that were covered included *Rhizopus*, *Mucor*, *Cunninghamella* and *Circinella*. Further investigation determined that the genus of *Rhizopus* produced the

most fumaric acid. *Rhizopus oryzae* is seen as the best fumaric acid producer since it has minimal excretions other than fumaric acid and can function aerobically or anaerobically (facultative anaerobe) (Martin-Dominguez *et al*, 2018; Odoni *et al*, 2017).

2.3.1 *Rhizopus oryzae*

Frits Went and Hendrik Coenraad Prinsen Geerligs first discovered *Rhizopus oryzae* ATCC 20344 in 1895. Although it has since been correctly renamed *Rhizopus delemar*, it is still referred to as *Rhizopus oryzae* in most literature (Abe *et al*, 2007). There are two groups of *Rhizopus oryzae*, namely a lactic acid-producing strain and a strain that produces fumaric acid and malic acid. The difference between the two strains is caused by the lack of lactate dehydrogenase, ldhA, in the fumaric acid-producing strain. The fumaric acid strain does contain ldhB but this enzyme is unable to produce sufficient lactic acid and this results in the production of fumaric acid and ethanol. This prompted the suggested name change to *Rhizopus delemar* by Abe *et al* (2007).

The production of fumaric acid by *R. oryzae* is sensitive to a variety of environmental conditions, the most influential being morphology, pH, nitrogen availability and metal ion concentrations (Papadaki *et al*, 2017; Roa Engel, Gulik, *et al*, 2011; Odoni *et al*, 2017; Y Zhou, Du, *et al*, 2000). Table 1 shows a list of studies that have worked on improving the fumaric acid production of *R. oryzae*. It can be seen that the titres produced in these studies range from $25.2\,\mathrm{g\,L^{-1}}$ to $103\,\mathrm{g\,L^{-1}}$ and the volume-based productivities range from $0.19\,\mathrm{g\,L^{-1}\,h^{-1}}$ to $1.21\,\mathrm{g\,L^{-1}\,h^{-1}}$. These results indicated that the highest titre was achieved with corn sugar (consisting mainly of glucose) and the highest productivity was achieved with immobilised fungal biomass.

2.3.2 Genetically modified *R. oryzae*

Since *R. oryzae* naturally produces fumaric acid, it is an obvious host on which to improve fumarate production. A reason why the production of fumaric acid has not switched to *R. oryzae* is that yields and productivity are currently higher with petrochemical synthesis. This has led to improving the production of *R. oryzae* through genetic engineering and metabolic engineering. Genetic engineering tools are effective with other microorganisms such as *Escherichia coli* and *Saccharomyces cerevisiae* (Jansen & Gulik, 2014). Random mutagenesis is one of these tools. The process works by randomly changing the genetics of the organism with chemicals, such as diethyl sulphate or nitrosoguanidine, or through radiation with ultraviolet light or gamma rays. The mutated organisms are then screened for the desired traits such as high fumaric acid yields (Q Xu, S Li, H Huang, *et al*, 2012).

Table 1: A literature compilation of the most prominent fumaric acid production studies with *R. oryzae* (Sebastian *et al*, 2019)

Carbon source	Reactor	Titre ($g\,L^{-1}$)	Productivity ($g\,L^{-1}\,h^{-1}$)	Reference
Corn sugar	Stirred tank	103	-	Rhodes *et al* (1962)
Glucose	Stirred tank	56.2	0.7	YQ Fu *et al* (2010)
Glucose	Stirred tank	41.1	0.37	L Huang *et al* (2010)
Glucose	Stirred tank	32.1	0.32	Kang *et al* (2010)
Glucose	Stirred tank	30.2	0.19	Roa Engel, Gulik, *et al* (2011)
Xylose	Shake flask	28.4	-	Wen *et al* (2013)
Xylose	Shake flask	45.3	-	Liu, W Wang, *et al* (2015)
Glucose/xylose	Shake flask	46.7	-	Liu, Zhao, *et al* (2017)
Corn straw	Shake flask	27.8	0.33	Q Xu, S Li, Y Fu, *et al* (2010)
Cornstarch	Shake flask	44.1	0.53	Deng *et al* (2012)
Cornstarch	Shake flask	45	0.55	L Huang *et al* (2010)
Brewery wastewater	Shake flask	31.3	-	Das & Brar (2014)
Apple juice waste	Shake flask	25.2	0.35	Das, Brar & Verma (2015a)
Dairy manure	Stirred tank	31	0.32	Liao *et al* (2008)
Glucose/glycerol	Shake flask	22.81	0.34	Y Zhou, Nie, *et al* (2014)
Synthetic medium	Immobilised	32.03	1.33	Gu *et al* (2013)
Synthetic medium	Immobilised	40.13	0.32	Naude & Nicol (2017)
Synthetic medium	Immobilised	30.3	0.21	Liu, Zhao, *et al* (2017)
Brewery wastewater	Immobilised	43.67	1.21	Das, Brar & Verma (2015b)

It has been found that mutants of *R. oryzae* are able to increase production parameters (Deng *et al*, 2012; Kang *et al*, 2010). However, Sebastian *et al* (2019) conducted a literature survey on mutant strains and compared their yields and productivities with those of pure cultures. They found that the mutant strains were not able to produce equivalent titres. Gene expression is another tool that has proved to be an effective strategy for improving production with microorganisms. B Zhang, Skory & Yang (2012) tested two gene modifications, namely the over-expression of endogenous pyruvate carboxylase and of exogenous phosphoenolpyruvate carboxylase. They found that pyruvate carboxylase over-expression had a negative effect on growth and the production of fumaric acid. Phosphoenolpyruvate carboxylase over-expression was, however, found to increase the yield on glucose by 26 % (B Zhang *et al*, 2012).

2.3.3 Other genetically engineered organisms

Industrial microbial workhorses like *E. coli* and *S. cereivisae* are well characterised and are ideal hosts for numerous different bioconversion steps. Accordingly these have

been studied to investigate the potential of producing fumaric acid. The understanding of the metabolisms of these organisms is of such depth that *in silico* simulations of their metabolism have been made (Sebastian *et al*, 2019). This understanding of their metabolisms has led to *S. cerevisiae* and *E. coli* being successfully modified to produce succinic acid and they are currently used commercially for succinic acid production (Jansen & Gulik, 2014).

E. coli has been genetically modified by deleting fumarase genes along with other genes that did not aid the fumarate production. Phosphoenolpyruvate carboxylase, a native enzyme in the reductive TCA cycle, was over-expressed and the rate of glucose uptake was improved by its replacement with a stronger gene. These modifications, along with others, led to a fumarate production of $28.2\,\mathrm{g\,L^{-1}}$ with a yield of $0.389\,\mathrm{g\,g^{-1}}$ at a productivity of $0.448\,\mathrm{g\,L^{-1}\,h^{-1}}$ (Song *et al*, 2013).

The use of *S. cerevisiae* is attractive since it has a better acid tolerance than *R. oryzae*. Acid tolerance is important in the production of fumaric acid since the pH of the medium has to be constantly corrected with a neutralising agent in order not to inhibit *R. oryzae* production (G Xu *et al*, 2013). Acid tolerance is beneficial since at low pH values the undissociated form of the acid will be produced and so will not require the addition of a neutralising agent (Taymaz-Nikerel *et al*, 2013). The use of a neutralising agent forms a large portion of production costs, especially since the fumarate salt has to be re-acidified before the fumaric acid can be removed. A study using a genetically modified strain of *S. cerevisiae* found that the insertion of reductive TCA enzymes and the over-expression of pyruvate carboxylase resulted in a fumaric acid titre of $5.64\,\mathrm{g\,L^{-1}}$ (G Xu *et al*, 2013). The yield of fumarate on glucose, however, is 20-fold lower than yields seen in similar fermentations with *R. oryzae*.

It can be seen from a comparison of these concentrations achieved with those of *R. oryzae* shown in Table 1 that the genetically modified strains are not yet able to produce equivalent titres or yields. However, it is clear that there is potential for genetic modification to make biological fumaric acid production possible, whether the organism is *E. coli* or a genetically modified strain of *R. oryzae*.

2.4 *Rhizopus oryzae* fermentation

2.4.1 Carbon metabolism

The metabolism of glucose by *R. oryzae* proceeds with glycolysis. The function of these enzymatic reactions is to break down glucose into two pyruvate molecules, which will be

further metabolised, and produce usable energy stores in the form of ATP and NADH. Pyruvate can then be metabolised through three pathways: the TCA cycle, ethanol production and the reductive TCA cycle used to produce fumarate. It is primarily transported into the mitochondria while producing an NADH and then decarboxylated to form acetyl-CoA, which is the entry to the TCA cycle. The TCA cycle forms a central part of the energy-producing metabolism of the cell. Pyruvate is metabolised through the TCA cycle to produce ATP, GTP, $FADH_2$, NADH and CO_2. ATP is the main energy store of a cell and is used for functions such as the production of fumarate or the transportation of fumarate out of the cell. GTP is structurally similar to ATP but is primarily used for protein synthesis. $FADH_2$ and NADH are both redox carrying molecules that are used in oxidative phosphorylation to produce ATP. NADH is also widely used in a variety of enzymatic reactions (Villadsen, Nielsen & Lidén, 2011).

Although the TCA cycle does contain fumarase, the enzyme responsible for producing fumarate, the fumarate excreted is from a fumarase isoenzyme that is part of the reductive TCA cycle in the cytosol. This was discovered by inhibiting the fumarase enzyme in the cytosol and observing a reduction in fumarate production. It has been found that there are two isoenzymes of fumarase present in the cytosol, one of which is also present in the mitochondria (Peleg *et al*, 1989). In another study the over-expression of the fumarase enzyme was investigated (B Zhang *et al*, 2012). It was found that fumaric acid production was replaced by the production of malic acid. This indicates that the fumarase enzyme may not be the root cause of fumaric acid production and that the production of fumarate is caused by the increased activity of a number of enzymes. Odoni *et al* (2017) conducted a metabolic analysis of *R. oryzae* under high and low fumarate-producing conditions. It was found that three enzymes (PYC, MDH, fumarase) in the reductive TCA cycle were over-expressed during high fumarate production. Another over-expressed enzyme was ASL, which forms a key part of the urea cycle. ASL and fumarase form a link from the TCA cycle to the urea cycle. The nitrogen-limited conditions of the fumarate production phase are seen to induce amino acid catabolism in *R. oryzae*. This increases the flux through the urea cycle and results in fumarate production.

The production of ethanol is primarily seen as a means of producing ATP under anaerobic conditions. However, ethanol is also produced aerobically. Under anaerobic conditions *R. oryzae* is unable to use oxidative phosphorylation to produce ATP from O_2 and has to use ethanol production to generate ATP. Oxidative phosphorylation forms part of the electron transport chain (ETC) that uses the redox potential of NADH and $FADH_2$ to generate ATP by converting O_2 to H_2O. The production of ethanol is an inefficient energy production since from one mole of glucose using ethanol-producing pathways only 2 moles of ATP can be formed compared with a possible 38 moles if the TCA cycle and ETC are used (Madigan *et al*, 2015).

Figure 4 shows a map of the metabolic pathways of *R. oryzae*. The anabolism of biomass shown has been simplified into one metabolic pathway from glucose. The production and consumption of NADH and ATP are represented by β and γ respectively. These values vary depending on the biomass formula and the environmental conditions (Villadsen *et al*, 2011). Glycerol is not produced by *R. oryzae* in large quantities and is only produced as a redox sink.

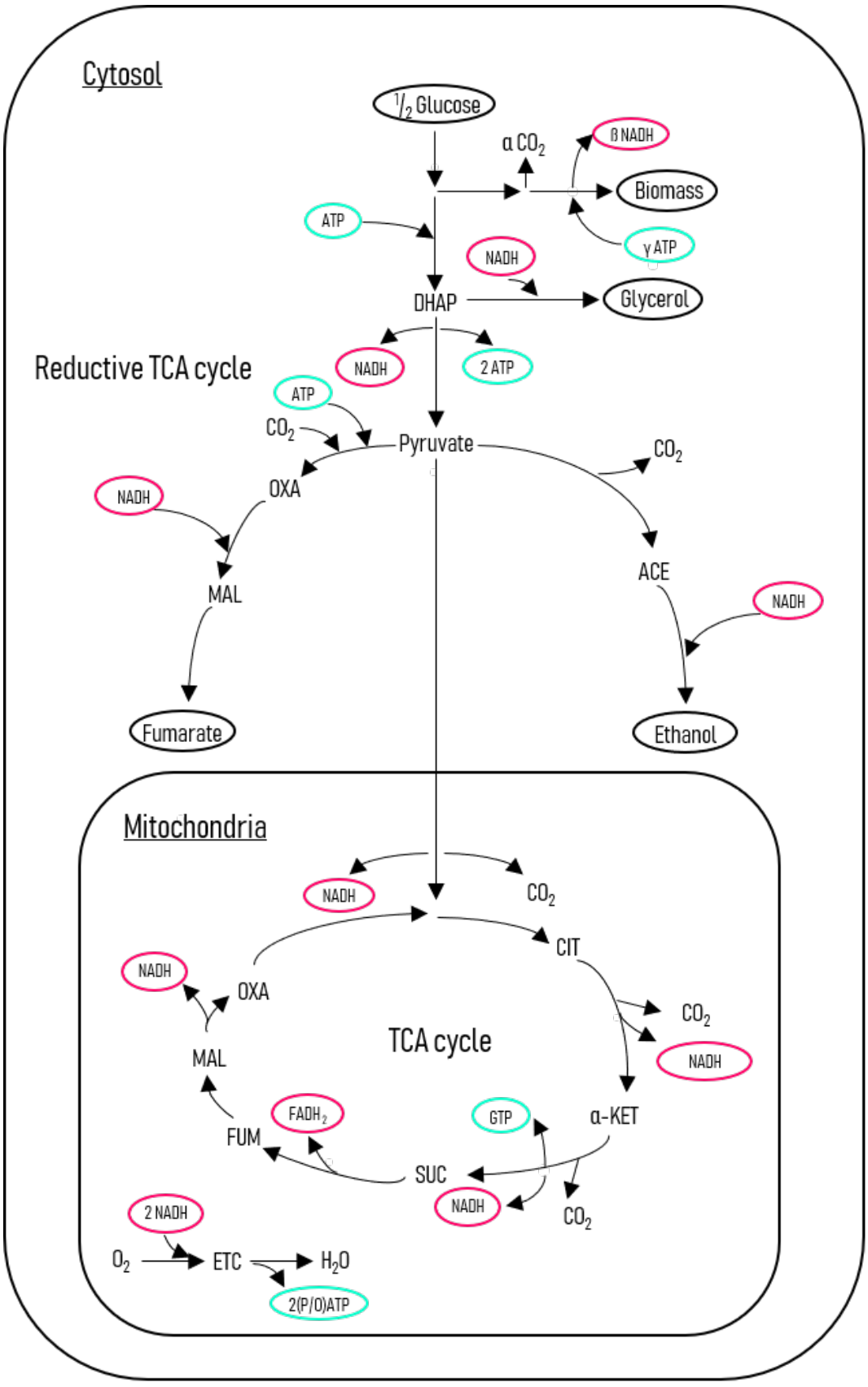

Figure 4: Metabolic pathways of *Rhizopus oryzae*

2.4.2 Acid transport

The excretion of fumaric acid into a medium is unlike that of alcohols since alcohols can diffuse passively through the cell membrane. Carboxylic acids require transporters to export them into the medium. There is an energy cost associated with this transport, which is dependent on the concentration of carboxylic acids already in the medium and on the pH of the medium. The reason for this cost is that the dissociated form of the carboxylic acids is exported and the H^+ ions also need to be exported against the proton motive force (Taymaz-Nikerel *et al*, 2013). The H^+ ions are transported out the cell using ATP synthase at the cost of one ATP per proton as illustrated in Figure 5. *E. coli*, a prokaryote, has an advantage over *R. oryzae*, a eukaryote, since it exports H^+ ions at a ratio of 3 H^+ to 1 ATP compared with 1 H^+ to 1 ATP. Depending on the pH of the medium a different transporter is used for the carboxylic acid. The three transporters and their associated methods are shown in Figure 5.

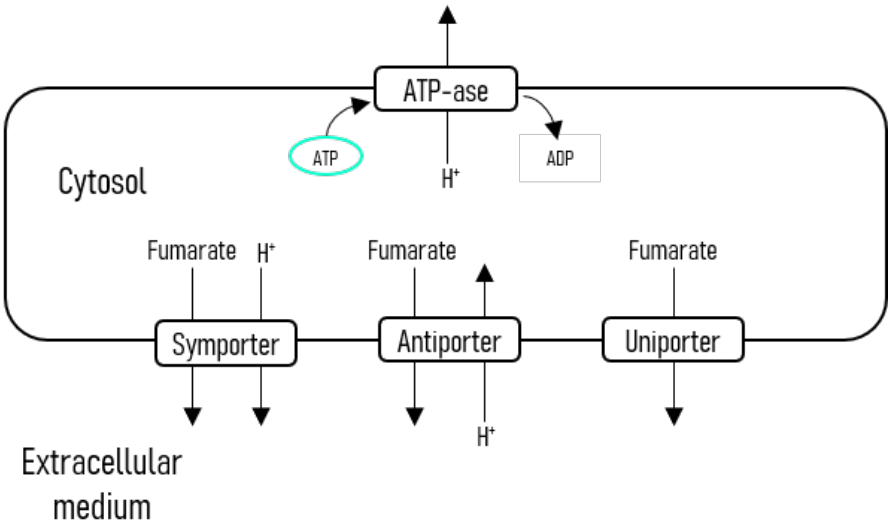

Figure 5: Illustration of dicarboxylic acid transport process

Equilibrium needs to be achieved between the fumaric acid concentration in the medium and that in the cell. This ratio is dependent on the pH of the medium and determines which transporter will be used at a specific pH. Figure 6 illustrates the relationship between the equilibrium concentration ratio and the pH for the three transporters. The dashed line is the ratio between the experimentally measured internal cell concentration ($10 \times 10^{-3}\,\mathrm{mol\,L^{-1}}$) and the economically viable medium concentration of $1\,\mathrm{mol\,L^{-1}}$ (Taymaz-Nikerel *et al*, 2013). The dashed line value decreases below a pH of 4 because the fumaric acid solubility decreases at low pH values. The transporter that is closest to the dashed line will most probably be used to transport fumarate out at the specific pH. A symporter provides the cheapest energy cost of 1 ATP per fumarate but is only able to

operate at high pH values around 7, whereas an antiporter can export fumarate at low pH values but costs 3 ATPs per fumarate.

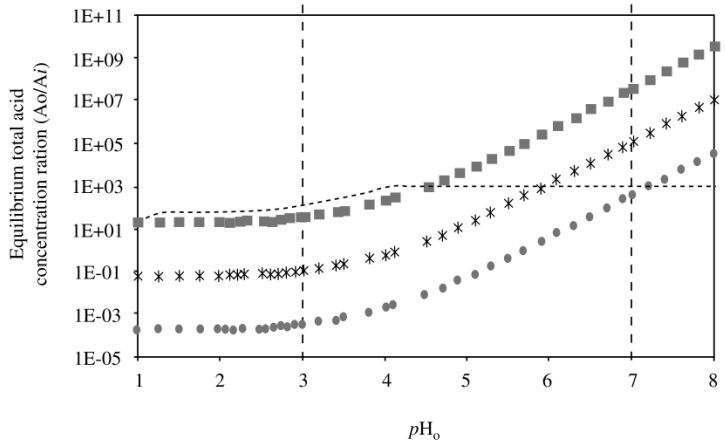

Figure 6: The equilibrium fumaric acid concentration ratio between the cell and medium, as a function of pH. Antiporter: squares, uniporter: stars, symporter: circles. The dashed line indicates the minimum internal cell concentration for export (10×10^{-3} mol L^{-1}) (Taymaz-Nikerel *et al*, 2013)

2.4.3 Fungal morphology

The morphology of *R. oryzae* can be greatly changed depending on factors such as shear, temperature, ion concentration and pH, to name only a few. This has resulted in many studies into the effect of morphology on the production of fumaric acid. The operation of the reactor determines the morphology and therefore has to be carefully chosen. Suijdam *et al* (1980) state that the reason for preferring a small pellet morphology over clumps or large pellets is that the mycelium can be easily removed from the medium, the medium can be easily aerated and mass transfer is improved. Figure 7 shows a comparison between a clump morphology and the ideal pellet morphology. It has been found that the diameter of the pellets is crucial to the fumaric acid yield on glucose (Z Zhou *et al*, 2011). It was concluded that the pellet formation is greatly affected by the pH, size of inoculum, glucose concentration and nitrogen content. It is also stated that large pellets or clumps can result in anaerobic zones in the mycelium matrix, which can result in the production of ethanol and lower fumaric acid yields. These claims have led to studies focused on the production of small pellets to increase mass transfer and reduce ethanol production (Y Zhou, Du, *et al*, 2000; Liao *et al*, 2007).

An immobilised biomass reactor is an alternative to pellet reactors. This alternative provides easier reactor operation since the biomass is not suspended in the medium, which means that the medium can easily be removed and replaced without the need for filtration. The use of immobilised biomass over pellets allows for continuous operation

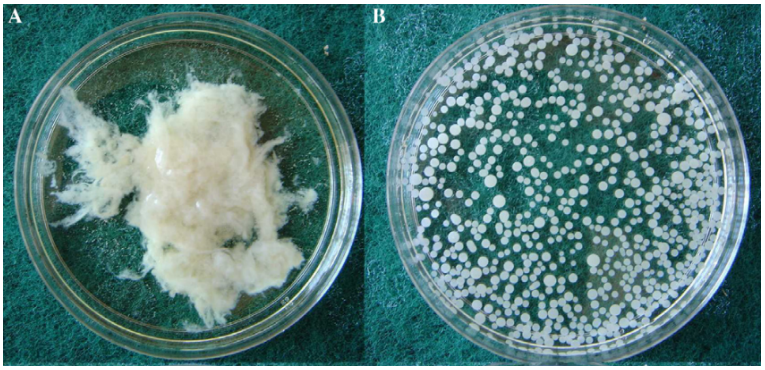

Figure 7: Morphology of fungal biomass: (A) clumps (B) pellets (adapted from Liao *et al* (2007))

since there is less chance of blockages from mycelium in the reactor (Naude & Nicol, 2018). Another benefit of the use of the immobilised biomass approach is the ability to grow biomass at a faster rate compared with the production of pellets. Pellet formation is promoted by using low spore inoculation concentrations and low metal ions concentrations in the medium (Liao *et al*, 2007; Suijdam *et al*, 1980). High concentrations of both factors promote the rapid growth of biomass.

2.4.4 Nitrogen supply and availability

The presence of nitrogen in the medium is crucial for the growth of *R. oryzae* since nitrogen is used to produce amino acids, which in turn make up the biomass and the enzymes used in all metabolism. *R. oryzae* is unable to fixate nitrogen from the atmosphere for growth. It is, therefore, vital that nitrogen is present in the medium in the form of urea, yeast extract or another protein complex (Madigan *et al*, 2015). The effect of the availability of nitrogen in the growth phase on fumaric acid production was investigated and it was found that low nitrogen concentrations negatively affected the biomass yield and the future fumaric acid production (Naude & Nicol, 2017). A high nitrogen content is crucial for healthy biomass growth.

It has been discovered that during the fumarate production phase the nitrogen content in the medium greatly influences the sustained production of fumarate. Naude & Nicol (2018) demonstrated that the rate of fumaric acid production can be sustained for longer periods by the addition of urea at a rate of $0.625\,\mathrm{mg\,L^{-1}\,h^{-1}}$. It was also observed that the yield of fumarate on glucose increased over the fermentation period up to a yield of $0.96\,\mathrm{g\,g^{-1}}$. This was attributed to the decline in ethanol production that was observed over a long continuous fermentation (400 h).

2.4.5 Neutralisation and separation of fumaric acid

Roa Engel, Straathof, *et al* (2008) suggested that a way of decreasing the production cost is to reduce the use of the neutralising agent used in the fermentation. Fumaric acid has pK_{a1} and pK_{a2} values of 3 and 4.5, respectively, and therefore small amounts can decrease the pH of the medium considerably. At low pH values, the production of fumarate is inhibited. This is commonly overcome by the addition of a neutralising agent to regulate the pH (Roa Engel, Gulik, *et al*, 2011). $CaCO_3$ has been found to produce high titres. However, the formation of calcium fumarate is undesirable since it increases the viscosity of the medium. Increasing the viscosity of the medium will have a negative effect on the nutrient uptake and oxygen mass transfer (Z Zhou *et al*, 2011). $NaHCO_3$ or NaOH are superior alternatives since they are more soluble than $CaCO_3$, which enables the biomass to be reused as precipitate does not build up in between the biomass, and downstream separation is easier (L Huang *et al*, 2010). Rhodes *et al* (1962) found no difference in the yields achieved with the three different neutralising agents, $CaCO_3$, KOH and NaOH. It was also found that sodium fumarate did have an inhibitory effect on the growth of biomass but not on the production of fumarate.

The separation of fumaric acid from the fermentation broth is an important yet overlooked factor. The fumaric acid that is produced by the respective organisms has to be either removed from the broth during fermentation using a selective membrane or neutralised. Ion-selective membranes have the ability to produce high titres, but have not found widespread use across the industry (Ilica *et al*, 2019). The use of NaOH for the neutralisation of fumaric acid has the possibility of producing very high titres because of the solubility of sodium fumarate and the fact that there is little to no inhibition of the salt on the organism. This process, however, does affect the downstream processing since there is a larger market for fumaric acid than for sodium fumarate. Acidification of the broth is therefore required, which involves a larger portion of the operating costs. Once the broth has been acidified, the low solubility property of fumaric acid aids the separation since a reduction in temperature can be used to crystallise fumaric acid out of the broth.

2.5 Crabtree effect

The Crabtree effect is a well-known phenomenon, initially discovered in *Saccharomyces cerevisiae* but which has also been found in numerous other microorganisms. The effect is described by the production of ethanol under aerobic conditions. Barford & Hall (1979) found that there was a limited respiration capacity in *S. cerevisiae* and once the glucose

feed rate surpassed this limit, ethanol production began. Figure 8a illustrates the general fermentation of *S. cerevisiae* at a low glucose concentration. CO_2 and biomass would be the only products since the amount of pyruvate produced is able to be consumed by the TCA cycle. If the glucose concentration is increased further past the threshold concentration, the effect shown in Figure 8 occurs. Here the high glucose concentration results in an increase in the glucose uptake rate, causing more pyruvate to be produced than can be consumed by the TCA cycle. This results in the production of ethanol as an overflow to avoid accumulation of pyruvate in the cell. The production of ethanol is unfavourable since it is often an unwanted by-product. In order to negate the ethanol, fed-batch fermentation has been utilised to increase the yield of biomass on glucose by maintaining a glucose-limited environment (Habegger *et al*, 2018). This strategy utilises the fact that ethanol production only starts at a glucose concentration above $150\,\mathrm{mg\,L^{-1}}$ (Verduyn *et al*, 1984). Therefore if the glucose concentration in the medium is maintained below the threshold value, for a Crabtree-positive organism, no ethanol should be formed.

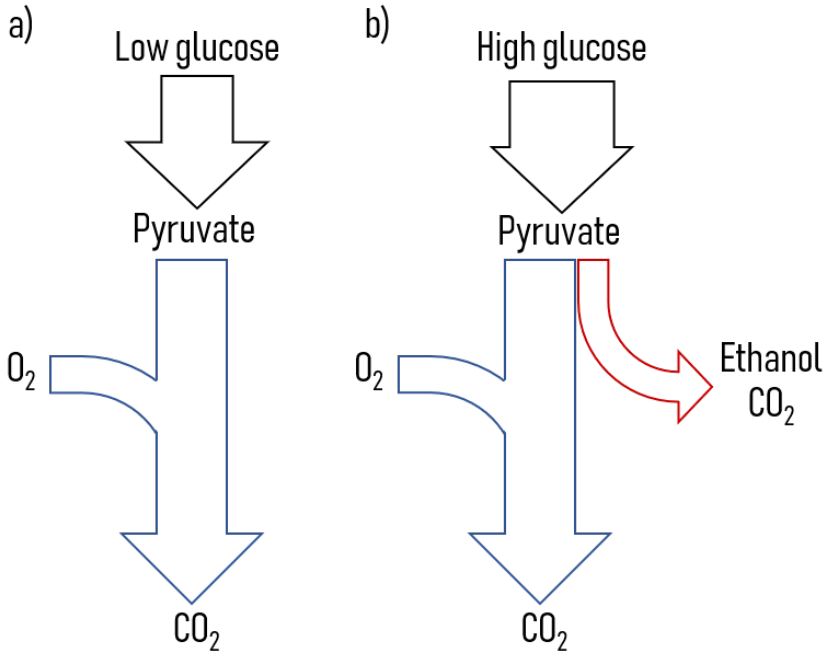

Figure 8: Illustration describing the Crabtree effect. a) The glucose concentration is below the threshold value. b) The glucose concentration is above the threshold value.

3 Experimental

3.1 Materials and methods

3.1.1 Microorganism

R. oryzae (ATCC 20344) was selected for the purposes of this study. This organism has been found to be the most successful at producing fumarate, as shown in the literature review.

3.1.2 Medium

Varying amounts of glucose and urea were added to a mineral medium for all fermentations. The mineral media contained (all of the following values have units of $g\,L^{-1}$): 0.6 KH_2PO_4, 0.25 $MgSO_4 \cdot 7\,H_2O$, 0.088 $ZnSO_4 \cdot 7\,H_2O$ and 0.005 $FeSO_4 \cdot 7\,H_2O$. Biomass was grown under batch conditions with $3.1\,g\,L^{-1}$ glucose and $2.0\,g\,L^{-1}$ urea (Naude & Nicol, 2017). The media for fed-batch growth of biomass contained the $2.0\,g\,L^{-1}$ urea but no glucose at the beginning of the fermentation as this was fed continuously at a rate of $0.07\,g\,L^{-1}\,h^{-1}$. The batch production fermentations contained $50\,g\,L^{-1}$ glucose and $0.1\,g\,L^{-1}$ urea. The fed-batch production fermentations began with only the mineral solution, then urea was fed at a rate of $0.625\,mg\,L^{-1}\,h^{-1}$ and glucose was fed at a rate between $0.131\,g\,L^{-1}\,h^{-1}$ to $0.329\,g\,L^{-1}\,h^{-1}$. In order to achieve low dilution rates, high-concentration solutions of both glucose and urea were made with $342\,g\,L^{-1}$ and $16\,g\,L^{-1}$, respectively. The dilution rate for the fed-batch production fermentations varied between $0.0018\,h^{-1}$ to $0.0027\,h^{-1}$, taking into account the glucose and urea additions, as well as the NaOH dosing. The urea solution incorporated the mineral solution to ensure that the mineral composition in the reactor remained constant throughout the experimental run. All the solutions were sterilised at 121 °C for 60 min. All chemicals used were obtained from Merck (Modderfontein, South Africa).

3.1.3 Reactor operation

The reactor design was adapted from a previous study which researched fumaric acid production with *R. oryzae* (Naude & Nicol, 2017). The reactor has a liquid volume of 1.08 L and a gas volume of 0.380 L. This design incorporates a textured polypropylene tube in the centre of the glass reactor tube, serving as an attachment surface for *R. oryzae* during the growth phase. Once the biomass has been grown, the immobilised fungus can

be rinsed with a mineral medium containing no nitrogen. The biomass produced has a thickness of approximately 1 mm to 2 mm and covers an area of 97.14 cm^2. The benefits of this system for biomass production over a mobilised pellet approach is that the thickness of the biomass can be closely controlled by means of the initial glucose concentration in the growth medium. Immobilised biomass also allows a simple sterile transition from growth to production conditions since the medium can be easily drained and replaced at the end of the growth phase. The switch to production requires rinsing of the biomass to remove residual nitrogen from the reactor. This was done by washing twice with the nitrogen-free mineral solution. Once this has been completed, the reactor is filled with the production phase medium and adjusted to a pH of 5. Growth and production fermentations were controlled at a pH of 5 using a 10 mol L^{-1}NaOH solution as a neutralising agent.

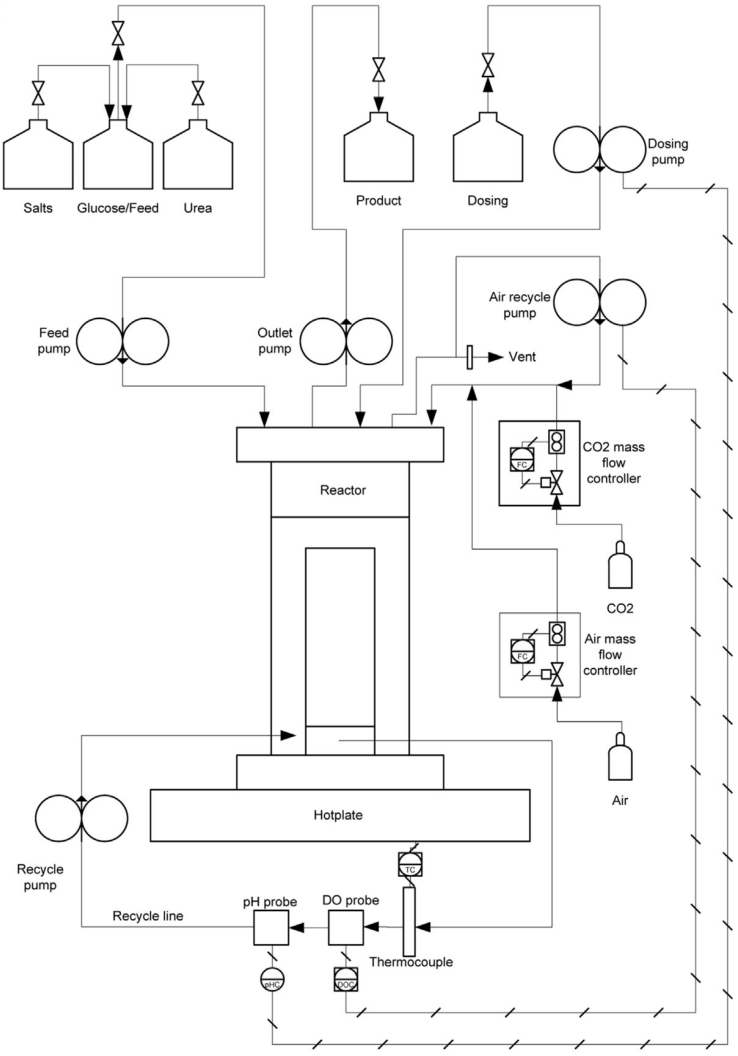

Figure 9: Process flow diagram of the reactor setup and control loops (Naude & Nicol, 2017)

The concentrated glucose and urea solutions were fed through 0.5 mm marprene tubing with the 120U Watson-Marlow (Johannesburg, South Africa) peristaltic pump. This allowed for fine control of the feed flow rate between 0.11 mL h^{-1} to 225 mL h^{-1} with

increments of 0.11 mL h^{-1}. The reactor was fed a gas mixture that consisted of 8 % CO_2, with 18.4 % O_2 and N_2 making up the complement, in all fermentations, unless otherwise stated. This mixture was controlled using an SLA5850 mass flow controller from Brooks (Hatfield, PA, USA). The CO_2 and O_2 compositions were checked and monitored online using a Tandem gas analyser 0588 from Magellan Biotech (Borehamwood, UK). The gas and liquid phases of the reactor were recycled to ensure that no concentration gradients were present, as described by Naude & Nicol (2017). The temperature of the reactor was maintained at 35 °C. The pH probe includes a temperature reading, which was used as an input into a PID controller. The reactor base was placed on a heating plate that was controlled by the PID controller. Figure 9 shows the process flow diagram of the reactor and the control loops in place to control the temperature, pH and DO.

3.1.4 Inoculum preparation

Once the reactor had been filled with the sterile growth medium, the reactor was operated without inoculating for 12 h. This was done to allow the gas composition out of the reactor to stabilise, the reaction temperature to be reached and the pH to be achieved. The spore inoculum used for batch growth fermentations had a spore concentration of 8×10^6 mL^{-1}, of which 10 mL were aseptically injected into the reactor through a silicon septum. The spore solution was prepared as follows: first potato dextrose agar plates were prepared and dried aseptically. It was found that a higher concentration of *R. oryzae* spores were produced per plate when moisture was removed from the PDA plates before their use. The plates were inoculated with a 50 % spore solution of glycerol and water that had been stored at −40 °C. The plates were then incubated at 35 °C for 3 d. The spores were suspended in distilled sterile water and rehydrated at 25 °C for 12 h. Slow growth rates were experienced if this final rehydration step was skipped.

3.1.5 Analytical methods

The fermentations were sampled at regular intervals over the period of the fermentation, with shorter experiments being sampled more frequently for a higher resolution. High Performance Liquid Chromatography (HPLC) was used to determine the concentrations of glucose, fumarate, ethanol, malic acid and succinic acid in the samples as described by Naude & Nicol (2017). The dry cell mass was determined at the end of each experimental run. The immobilised biomass was removed from the polypropylene tube and centrifuged at 2000 rpm for 10 min, the supernatant was re-suspended in distilled water and the biomass was then centrifuged again. This was repeated a total of three times. The biomass was finally dried at 70 °C for 48 h before being weighed.

HPLC analysis is not instantaneous and therefore it is not possible to determine the glucose concentration in the reactor online. Consequently, it is not possible to know whether or not the growth fermentation has reached completion. However, the online CO_2 outlet concentration is available. On the assumption that the gas volume into and out the reactor remains constant, the concentration is employed to calculate the CO_2 gas production rate using Equation 1. The a full nomenclature list can be found here.

$$r_{CO_2} = \frac{1}{V}\left(Q_{gas}(C^o_{CO_2} - C_{CO2}) - V_g\frac{dC_{CO2}}{dt}\right) \tag{1}$$

3.2 Model and analysis

3.2.1 Batch growth of immobilised fungus

The biomass growth curve could not be determined experimentally since only one data point of the biomass concentration could be determined per run. A model of the biomass growth was therefore developed that would determine the growth curve based on the limited data. The data used to fit the model included the HPLC-determined concentration profiles of glucose and the metabolite products, as well as the final biomass concentration. The growth curve was fitted assuming exponential growth and Monod growth characteristics (Villadsen *et al*, 2011). The Monod model (Equation 2) predicts a low-concentration regime where substrate uptake rates are proportional to substrate concentration. This affects the growth rate proportionally but only comes into affect towards the end of the batch fermentation as the glucose becomes depleted. Constant yield coefficients were assumed for the metabolites on glucose. These yields were used in conjunction with the total mass balance equation (Equation 3) to solve the mass balance for all the rates. The chemical equation uses glucose, O_2 and urea as reactants and biomass, CO_2, H_2O, fumaric acid, succinic acid, ethanol, glycerol, malic acid and pyruvic acid as the products. The calculated production and consumption rates were then used within Equation 4 in an Euler integration loop to determine the change in concentration for every time step. To fit the model to the data and determine the growth rate, LMFIT, a module within the Python environment, which uses a non-linear least-squares minimisation algorithm, was then used. The parameters varied to obtain a reasonable fit include the μ_{max}, K_m and the yield of biomass on glucose.

$$r_x = \mu_{max}\frac{C_g}{C_g + K_m} \tag{2}$$

$$C_6H_{12}O_6 + Y_{SO}O_2 + Y_{SU}CH_4N_2O \rightarrow$$
$$Y_{SX}CH_{1.8}O_{0.5}N_{0.2} + Y_{SC}CO_2 + Y_{SH}H_2O + Y_{SF}C_4H_4O_4 + Y_{SSu}C_4H_6O_4 \quad (3)$$
$$+Y_{SM}C_4H_6O_5 + Y_{SE}C_2H_6O + Y_{SG}C_3H_8O_3 + Y_{SP}C_3H_4O_3$$

$$\frac{dN_i}{dt} = r_i \cdot C_x \cdot V \quad (4)$$

3.2.2 Fed-batch fermentations

To determine the production rates and yields of fumarate or other metabolites, a mass balance was conducted over the reactor. The HPLC-determined concentration profiles were interpolated to determine instantaneous rates, and these rates were then input into Equation 5, which was solved using Euler integration. The same mass balance described for the batch fermentation model was used. This allowed the calculation of the instantaneous and accumulative yields.

$$\frac{dN_i}{dt} = Q_o C_i^o - QC_i + r_i C_x V \quad (5)$$

4 Results and discussion

4.1 Growing biomass in excess glucose

The immobilised biomass for all the fermentations was grown with excess nitrogen. Once the growth phase was complete, the reactor medium was switched to a nitrogen-limited solution to induce the production of fumarate. The completion of the growth phase was determined by the CO_2 production rates. As growth begins, CO_2 is produced as a by-product from the consumption of glucose. The rate of biomass production is exponential and in turn results in an exponential production of CO_2. These rates are proportional since the ATP consumed for the production of biomass is generated by the production of CO_2 through respiration. The CO_2 production rate reaches a peak, after which the rate falls steadily, which is an indication of total glucose consumption. HPLC analysis is used to corroborate the glucose concentration in the medium.

Figure 10 illustrates the metabolite profiles obtained from two growth phase fermentations. These experiments were done to prove the repeatability of the biomass growth process. The fermentations were found to reach full glucose consumption ($3.1\,\mathrm{g\,l^{-1}}$) within 25.6 ± 1.8 h. The growth period was consistent for all fermentations unless NaOH was used in the initial pH correction, the addition of NaOH caused a lag in the growth rate. The yield of biomass on glucose was found to be $0.196 \pm 0.033\,\mathrm{g\,g^{-1}}$. A model was fitted to estimate the specific growth rate of *R. oryzae*. The model used fixed yield coefficients of ethanol and fumarate on glucose to obtain a suitable fit. Their values were 0.211 and 0.058 respectively. The estimated specific growth rate was found to be $0.255\,\mathrm{h^{-1}}$.

The profiles in Figure 10 show that growth is initially slow to start as a result of the time that is taken for the sporulation of the inoculated spores. After this period the consumption rate of glucose increases rapidly, with a visible accumulation of biomass in the reactor. It can be seen that both ethanol and fumarate are the main by-products during the fermentation. Malic acid, pyruvic acid and succinic acid were produced in trace concentrations. The yield of ethanol on glucose is higher than the yield of biomass on glucose. This is possibly an indication of the Crabtree effect. This is likely since ethanol is produced in an aerobic environment, which indicates that *R. oryzae* may have a limited capacity for respiration. When the glucose consumption surpasses this capacity, ethanol production is triggered as an overflow of carbon. The ATP generated as a result of the ethanol produced (1 mole ATP per mole ethanol produced) coincides with the amount of ATP required to transport the fumarate produced out of the cell (3 ATP per mole of fumarate). Fumarate is not usually produced in a nitrogen excess environment which suggests that it was only produced as a means of consuming the excess ATP,

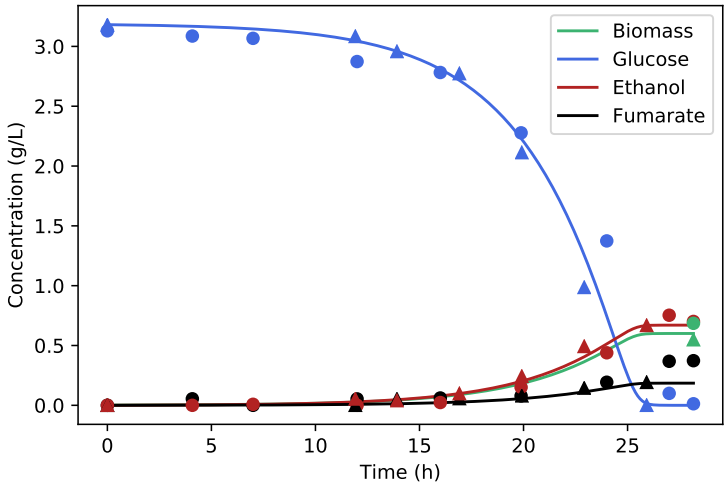

Figure 10: Repeat profiles of metabolite accumulation under growth conditions using 3.1 g/L of glucose and nitrogen excess. Notable production of ethanol and fumarate was observed, with 0.62 $\pm$ 0.097 $\mathrm{g\,L^{-1}}$ of biomass obtained at the end of the run. The fitted model indicates biomass accumulation up to the final measured point. The model employed fixed yield coefficients of ethanol and fumarate on glucose (Y_{SE}= 0.211 And Y_{SF}= 0.058). The estimated maximum specific growth rate was found to be 0.255 $\mathrm{h^{-1}}$ and the Monod constant was 0.176 $\mathrm{g\,L^{-1}}$.

produced through ethanol production.

4.2 Fumarate production with DO variation

The results presented above suggest that *R. oryzae* may be a Crabtree-positive organism. The literature suggests that the production of ethanol is a result of anaerobic zones that develop in the mycelium matrix (Y Zhou, Du, *et al*, 2000; Suijdam *et al*, 1980). This is contrary to explanation of the Crabtree effect. To evaluate the validity of the effect of anaerobic zones on the production of ethanol an experiment was conducted in which two batch production fermentations were done at different dissolved oxygen values (DO). The DO values were 18.4 % to 85 %. This significant difference was selected to ensure that anaerobic zones would be eradicated at the higher DO and an effect would be seen in the ethanol production. The 4.6-fold increase of the DO is assumed to increase the oxygen mass transfer and in turn supply more oxygen to the cell, reducing the need for ATP produced from ethanol production.

The results of the experiment can be seen in Figure 11. The biomass used in this experiment was grown with the same procedure as was described from Figure 10. This growth procedure produced biomass that had a thickness of approximately 1 mm to 2 mm. It is state in the literature that this thickness is the ideal pellet diameter to reduce the

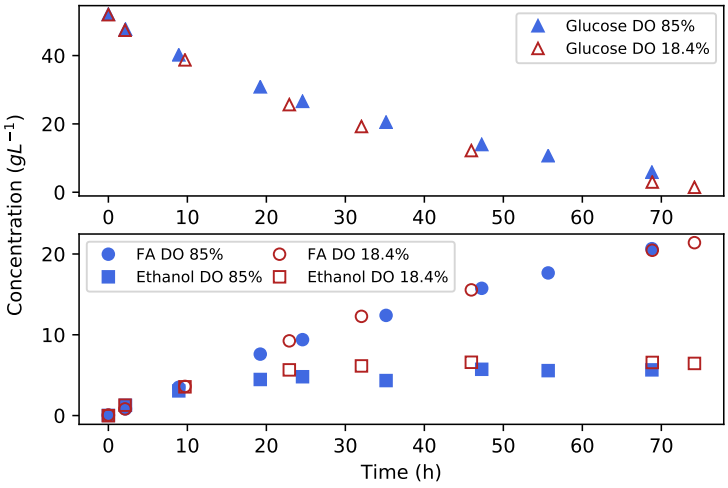

Figure 11: The effect of DO on fumarate production where $50\,\mathrm{g\,L^{-1}}$ of glucose was initially used. The DO was varied from 18.4 % to 85 %. A negligible difference was observed between the two runs.

formation of anaerobic zones (Y Zhou, Du, *et al*, 2000; Z Zhou *et al*, 2011). The results in Figure 11 show that the concentration profiles of glucose, ethanol and fumarate are equivalent, indicating no effect of DO on the ethanol production.

This suggests that the anaerobic zones do not play a role in the production of ethanol and most likely do not exist. Ethanol produced from mycelium with a thickness of 2 mm or less can therefore not be attributed to the lack of oxygen supply. This finding supports the hypothesis that *R. oryzae* is a Crabtree-positive organism since oxygen availability is unrelated to the production of ethanol.

4.3 Manipulating glucose uptake rates under growth conditions

The results presented so far offer good support for *R. oryzae* being Crabtree-positive. The production of ethanol is a result of the excess availability of glucose in the medium. Ethanol produced aerobically by *S. cerevisiae* can be negated by controlling the glucose uptake rate (Aiba, Nagai & Nishi, 1976). This gives the organism the ability to maximise its glucose uptake and exceed its respiratory capacity. Ethanol is then produced as an overflow mechanism to remove the excess carbon that cannot be metabolised through the TCA cycle. A glucose uptake regime exists where the uptake rate is proportional to the glucose concentration in the medium. This was first described by Monod. Once the glucose concentration surpasses a limit, the organism reaches a maximum uptake rate (Fogler, 2006; Habegger *et al*, 2018). To further test the metabolic characteristics of *R. oryzae* an experiment was conducted in which biomass was grown in a glucose-limited

but nitrogen excess environment. This was done using a fed-batch reactor where the glucose feed rate could be closely controlled.

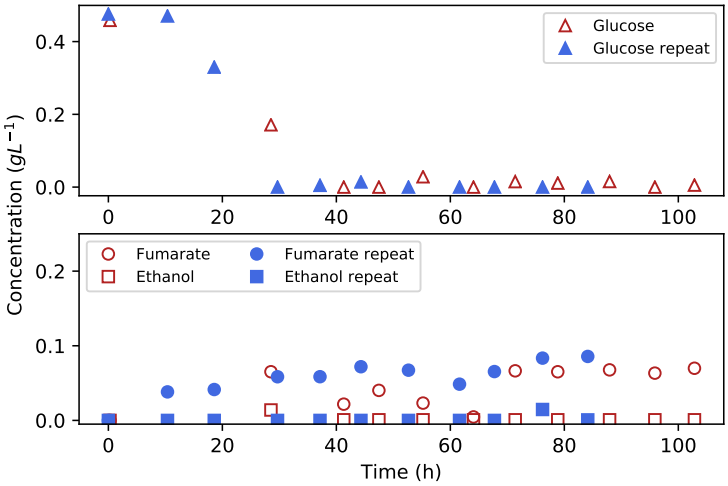

Figure 12: Glucose, ethanol and fumarate concentrations during fed-batch growth of *R. oryzae*. Glucose was added at a constant rate of $0.07\,\mathrm{g\,L^{-1}\,h^{-1}}$. All concentrations approximate zero, except glucose in the initial stages of the experiment. Ethanol overflow was clearly avoided.

Figure 12 shows the concentration profiles of the glucose fed-batch growth fermentation. The fermentation began with no initial glucose before inoculation. Glucose was then fed at a rate of $0.07\,\mathrm{g\,L^{-1}\,h^{-1}}$ for the duration of the fermentation. There was an initial glucose accumulation as a result of the time taken for the sporulation to occur. The glucose was then depleted once the biomass concentration increased. Thereafter, the glucose concentration remained at zero for the rest of the fermentation. Fumarate was only produced during the period of high glucose concentration and the concentration remained constant for the remainder of the fermentation. Ethanol was not produced at all during the fermentation, indicating that the glucose uptake rate that results in ethanol overflow was never reached.

R. oryzae responded to a limited glucose fermentation similar to that of *S. cerevisiae*. This indicates that the Crabtree mechanism probably present in *R. oryzae* can be utilised to negate the parallel production of ethanol and increase the yield of fumarate on glucose.

4.4 Manipulating the glucose supply under production conditions

Thus far evidence has been found that indicates Crabtree-positive characteristics of *R. oryzae*. However, the results have focused on the growth of biomass and not on the more valuable production of fumarate. Therefore the Crabtree response needs to be tested during the production phase during which the nitrogen concentration is limited. The Crabtree effect is expected to function similarly during the production of fumarate to what it would during the production of biomass with *S. cerevisiae*. This is likely since the production of biomass consumes ATP in the same way as does the export of fumarate from the cell assuming that the cause of ethanol production is overflow. To test whether the ethanol can be negated from the production of fumarate, a fermentation was conducted in which a glucose feed rate of $0.07\,\mathrm{g\,L^{-1}\,h^{-1}}$ was used. Figure 13 shows the results for the fermentations in this section. These are similar to the biomasses for the fermentations shown in Figure 10. It can be seen that there was no metabolite production for the first 80 h of the fermentation. The final yield of fumarate on glucose was found to be only $0.162\,\mathrm{g\,g^{-1}}$. This suggests that the glucose feed rate was too low resulting in most of the glucose being used for cell maintenance and for the transition from growth metabolism to fumarate production metabolism. The transition period was longer than expected since a normal batch fermentation experienced a transition of approximately 20 h until fumarate production began. Because of this long transition period, it was decided to increase the feed rate to $0.131\,\mathrm{g\,L^{-1}\,h^{-1}}$ to decrease the transition period. With this increase fumarate production began after 20 h and therefore this rate was used as the base for the subsequent experiments.

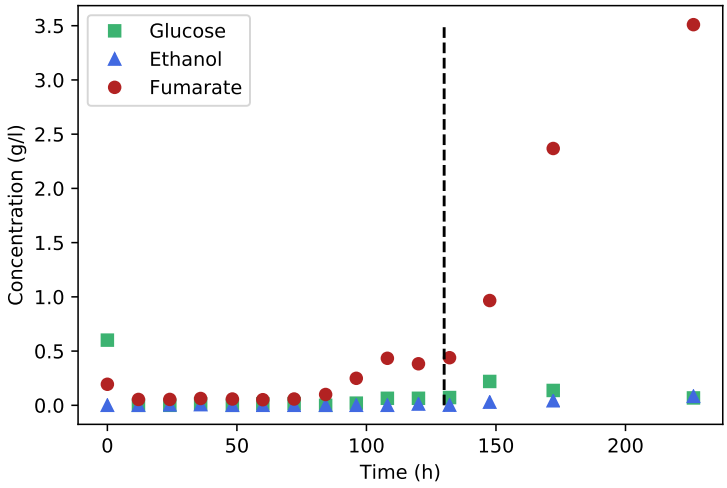

Figure 13: Concentration profiles of a production fermentation illustrating a slow transition to fumarate production. The initial glucose feed rate was $0.07\,\mathrm{g\,L^{-1}\,h^{-1}}$ and then at 130 h the feed rate was increased to $0.131\,\mathrm{g\,L^{-1}\,h^{-1}}$ which resulted in a substantial increase in the production rate.

Two production fermentations were conducted for approximately 200 h with different glucose feed rates. The two fermentations employed two different feed strategies, as can be seen in Figure 14. The fermentations began at the base feed rate of $0.131\,\mathrm{g\,L^{-1}\,h^{-1}}$ and after 66 h both were stepped up to a feed rate 50 % higher ($0.197\,\mathrm{g\,L^{-1}\,h^{-1}}$). Run 1 remained at this feed rate for the duration of the fermentation, while the feed rate of run 2 was stepped up a further 2 times, as can be seen in Figure 14. The concentration profiles of fumarate, ethanol and glucose are shown in Figures 15, 16 and 17 respectively.

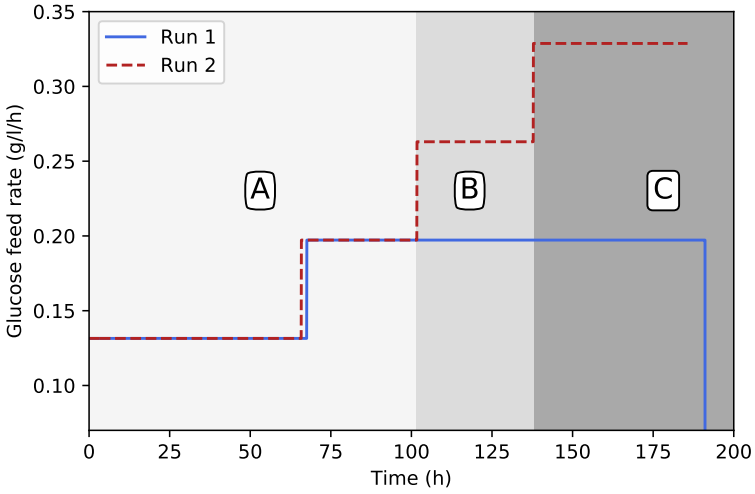

Figure 14: Glucose dosing rates for run 1 and 2. The dosing rate of run 1 was increased by 50 % once. Towards the end of the fermentation, dosing was stopped and the glucose concentration was depleted. The dosing rate of run 2 was increased three times by 50 % of the original rate.

Comparison of the first 100 h of the fermentation profiles (Figure 14) shows it can be seen that they are essentially a repeat and confirm the validity of the observed responses. The main observation from these results is that there was no ethanol produced at a glucose feed rate of 0.197 g L^{-1} h^{-1} in run 1. This shows that ethanol production can be avoided with glucose control while fumarate is still produced. The response of ethanol production within the first 25 h indicates the transition period from growth metabolism to fumarate production. The glucose feed rate was still at the lower base feed rate during this transition. It can be seen that in both fermentations ethanol consumption begins after 25 h. This suggests that once the metabolism has fully transitioned to production, a feed rate of 0.131 g L^{-1} h^{-1} is still below the respiratory capacity limit since ethanol can be metabolised along with the glucose fed. This feed rate is therefore below the glucose uptake rate that would induce ethanol overflow.

Run 1 obtained a sustained fumarate production rate of 0.15 g L^{-1} h^{-1} from the glucose feed rate of 0.197 g L^{-1} h^{-1} while producing no ethanol. Looking at Figure 17 one can see that the glucose concentration increases and then stabilises around 0.28 g L^{-1} while no ethanol is produced. This indicates that the glucose concentration is below the threshold glucose concentration that would induce ethanol overflow. This value is in close agreement with the 0.15 g L^{-1} of *S. cerevisiae* (Verduyn *et al*, 1984). The results of the run provide good evidence for the Crabtree-positive nature of *R. oryzae* and indicate that close control of the glucose addition can negate the unwanted production of ethanol.

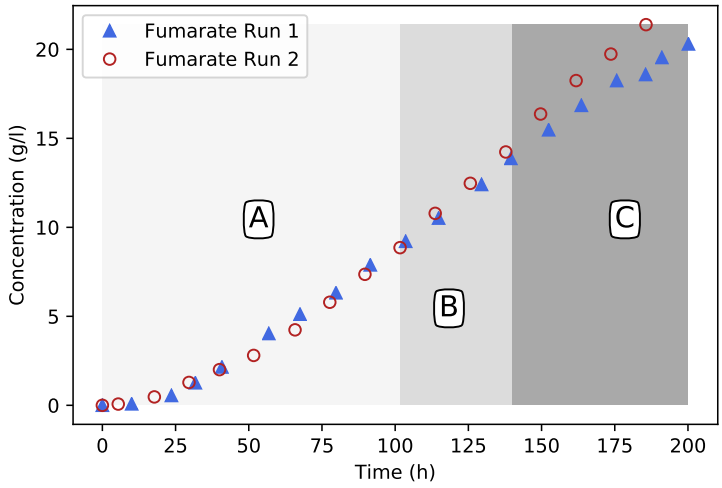

Figure 15: Fumarate production profiles for runs 1 and 2. Note the slight increase in fumarate excretion rates in regimes B and C.

To further test the metabolic responses of *R. oryzae*, in run 2 the glucose feed rate was increased above the ethanol overflow point and the maximum glucose uptake rate. Comparison of run 1 and 2 shows that they only begin to deviate once the glucose feed rate is increased to $0.263\,\mathrm{g\,L^{-1}\,h^{-1}}$ for run 2. To simplify the comparison between the two runs, they have be divided into three sections: A, B, and C. Section A represents that period where the feed rate of the runs was identical, section B is where run 2 had a 33 % higher feed rate than run 1, and section C is where run 2 had a 67 % higher feed rate than run 1.

The major difference between runs 1 and 2 begins in section B where the ethanol profiles differ (see Figure 16). It can be seen that once the glucose feed rate was increased to $0.263\,\mathrm{g\,L^{-1}\,h^{-1}}$, the ethanol overflow point was surpassed and ethanol production began. This indicates that the respiration capacity of the cell was exceeded and the cell could no longer accommodate all the carbon metabolised by the glycolytic pathways through respiration or fumarate production. Accumulation of carbon in the cell is unwanted and it was therefore excreted as ethanol. Comparison of the glucose profiles of the runs in section B shows that they have similar concentrations. This indicates that the feed rate is still below the glucose uptake maximum and that most of the glucose feed was metabolised. The glucose concentration value of $0.28\,\mathrm{g\,L^{-1}}$ can be regarded as a threshold value, below which all glucose can be consumed. Section C of Figure 17 clearly shows that once the glucose feed rate was increased, glucose accumulation began and the concentration quickly surpassed $0.28\,\mathrm{g\,L^{-1}}$.

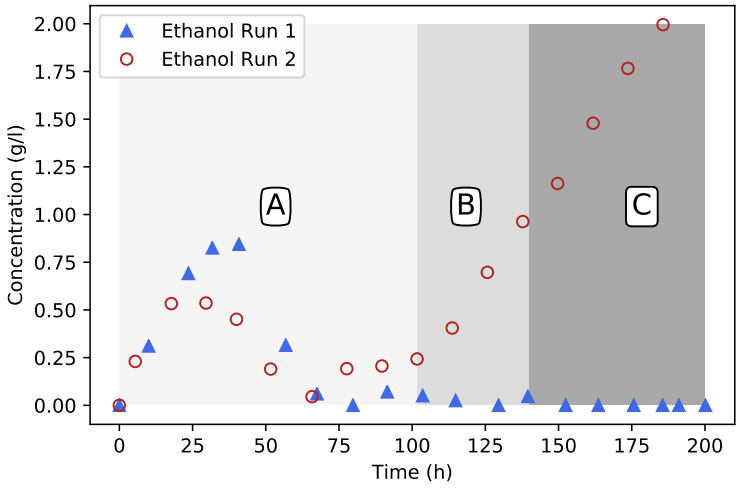

Figure 16: Ethanol profiles for run 1 and 2. Beyond the first 25 h transition phase, no ethanol overflow is observed in run 1. Run 2 exhibits clear ethanol overflow in regimes B and C where glucose addition rates were increased.

The fumarate concentration profiles show that once the feed rate was increased in section B for run 2, the fumarate production rate increased. This increase in production rate is more clearly seen in section C where the concentrations of the two profiles separate. This result indicates that the glucose feed rate of run 1 in sections B and C was lower than the maximum uptake rate before ethanol overflow. Theoretically, this means that a glucose feed rate higher than $0.197\,\mathrm{g\,L^{-1}\,h^{-1}}$ can be fed while ethanol production is maintained at zero. This glucose feed rate can be calculated by assuming the that yield of fumarate on glucose will remain the same before and after ethanol overflow has begun. The fumarate production measurements are then used to calculate the amount of glucose that will be required to produce an equivalent amount, provided ethanol overflow is not reached. This glucose feed rate was found to be $0.244\,\mathrm{g\,L^{-1}\,h^{-1}}$.

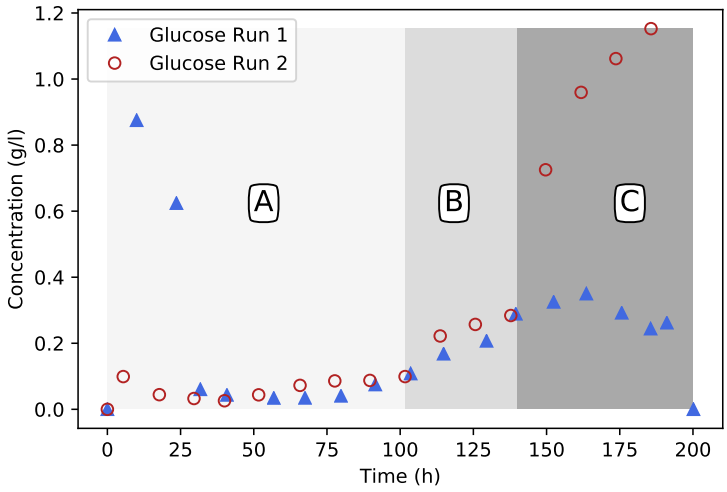

Figure 17: Glucose profiles for run 1 and 2. Glucose breakthrough observed for run 2 in regime C, where glucose addition rates exceed glucose consumption rate.

In section C of run 2, the glucose feed rate was increased to $0.329\,\mathrm{g\,L^{-1}\,h^{-1}}$. It can be seen from Figures 15 and 16 that the production rates of both ethanol and fumarate increased only slightly. This implies that the feed rate surpassed the maximum glucose uptake rate and that the maximum lies somewhere between $0.263\,\mathrm{g\,L^{-1}\,h^{-1}}$ and $0.329\,\mathrm{g\,L^{-1}\,h^{-1}}$. The glucose that was not consumed accumulated in the medium (see Figure 17). However, not enough information is available at present to determine a single value for the maximum glucose uptake rate. This can be resolved in further studies.

As can be seen from Table 1, productivities are commonly reported on a volumetric basis in literature. However, when reporting the maximum glucose uptake rate and the threshold glucose uptake rate before ethanol breakthrough, the preference is to report the rates on a biomass basis. The drawback of using biomass rates is that the biomass can only be quantified once the fermentation has reached completion. Runs 1 and 2 were found to have biomass concentrations of $2.49\,\mathrm{g\,L^{-1}}$ and $2.51\,\mathrm{g\,L^{-1}}$, respectively. These concentrations differ greatly from the biomass concentration measured ($0.617\,\mathrm{g\,L^{-1}}$) after the biomass growth phase as shown in Figure 10. The same method was used to produce the biomass used in runs 1 and 2. This indicated that there was a four-fold increase in biomass, which is unexpected since the production phase is nitrogen-limited and the total urea fed over the production period was only $0.116\,\mathrm{g\,L^{-1}}$. Based on the general biomass formula $CH_{1.8}O_{0.5}N_{0.2}$ (Villadsen *et al*, 2011), additional protein synthesis as a result of urea will only contribute 4 % of additional biomass and cannot explain the considerable increase in mass. It is suspected that the increase in biomass is a result of carbohydrate stores and not the production of metabolically active biomass. Given this, we have based the following rates on the biomass concentration obtained directly after the growth

period since the enzymatic protein content responsible for the metabolism was more concentrated for this biomass. Accordingly, the ethanol breakthrough rate is calculated to be $0.395\,\mathrm{g\,g^{-1}\,h^{-1}}$, while the glucose breakthrough rate lies between $0.426\,\mathrm{g\,g^{-1}\,h^{-1}}$ and $0.533\,\mathrm{g\,g^{-1}\,h^{-1}}$.

Towards the end of run 1 a yield of $0.802\,\mathrm{g\,g^{-1}}$ fumarate on glucose was obtained; this was over 50 h. The yield over the entire fermentation period was $0.713\,\mathrm{g\,g^{-1}}$ since fumarate was not produced during the first hours of the fermentation. The yield for run 2 during the highest glucose feed rate was found to be $0.596\,\mathrm{g\,g^{-1}}$. This translates to run 1 having a $0.206\,\mathrm{g\,g^{-1}}$ better yield as a result of controlling the glucose addition below the ethanol breakthrough rate. It also illustrates the effectiveness of the fed-batch reactor operation and the extent of carbon losses to ethanol that occur under batch conditions. These yields were calculated by accounting for all fumarate produced over the period and for the amount of glucose added to the reactor.

4.5 Future exploration to optimise fumarate production

The work presented thus far has been written up in a paper and has been submitted to *Biotechnology for Biofuels*. The paper is currently under review. The focus of this thesis thus far has been on minimising ethanol production, the Crabtree effect and manipulating the glucose feed rate in order to observe the response of *R. oryzae*. There are numerous factors affecting the production of fumarate, as can be seen from the literature review presented in Section 2.1. Major factors are the pH of the medium, the urea content and/or feed rate, the metal ion composition and the addition of more complex protein sources (Taymaz-Nikerel *et al*, 2013; Naude & Nicol, 2018; Y Zhou, Du, *et al*, 2000; K Zhang, Yu & Yang, 2015). Operation of the reactor is another field that shows promise when considering the present work as well as other studies that focus more on the type of reactor used, the gas composition fed and alternative immobilisation strategies (Sebastian *et al*, 2019; Cao *et al*, 1997; Roa Engel, Gulik, *et al*, 2011). All these factors can greatly affect the fumarate production and metabolism of *R. oryzae*. For the successful production of fumaric acid biologically on an industrial scale, all these aspects have to be optimised to compete with the years of development that have gone into the petrochemical production of fumarate. The following results are an initial experiment that will form part of further publications.

The initial investigation will be into the effect of the nitrogen feed rate on the production of fumarate. It has been found that the production of fumarate through the reductive TCA cycle is closely linked to the urea cycle: it is induced by increased activity of the urea cycle. It is suggested that a high carbon:nitrogen ratio is crucial for the activation

of these cycles. High carbon:nitrogen ratios can be easily controlled by manipulating the feed rate of urea into the system. This has been shown by Naude & Nicol (2018) to affect the fumarate production stability and to increase the yield over time. A feed rate of $0.625\,\mathrm{mg\,L^{-1}\,h^{-1}}$ was found to produce stable fumarate production rates, while decreasing the yield of ethanol over time. At a feed rate three times higher, it was found that the fumarate production increased over time. The next step to optimise the environmental conditions of the reactor for fumarate production was to double the urea feed ($1.25\,\mathrm{mg\,L^{-1}\,h^{-1}}$) in order to determine the effect of an increased nitrogen feed rate on fed-batch conditions. The same glucose feed rate profile as in run 2 shown in Figure 14, was used for run 3. The concentration profiles produced from the fermentations are shown in Figures 18, 19 and 20.

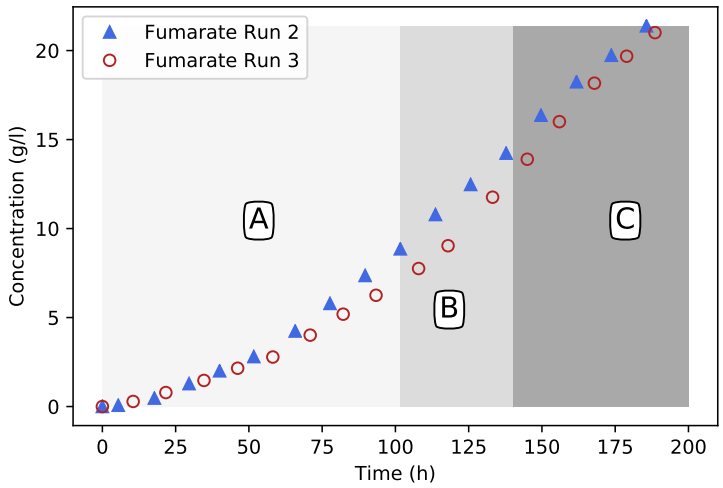

Figure 18: Fumarate production profiles for run 2 and 3. Run 3 has a lower fumarate production rate in sections A and B, but in section C the rate increases.

The fumarate concentration profiles are shown in Figure 18. It can be seen that initially, the production rates are equivalent. Towards the end of section A, the rates begin to diverge and run 1's (higher carbon: nitrogen ratio) rate is higher than that of run 3. The difference in production rates is sustained in section B. The lower production rates of run 3 may be due to the inhibitory effect of nitrogen on fumarate production. However, the variation in concentrations is not all that large and may be due to inconsistencies in the fermentations. In section C it can be seen that the production rate for run 3 increases and the final concentrations achieved for the two runs is equivalent. Comparison of the overall profiles shows that they are not substantially different the variations are not large enough to attribute to any definitive cause.

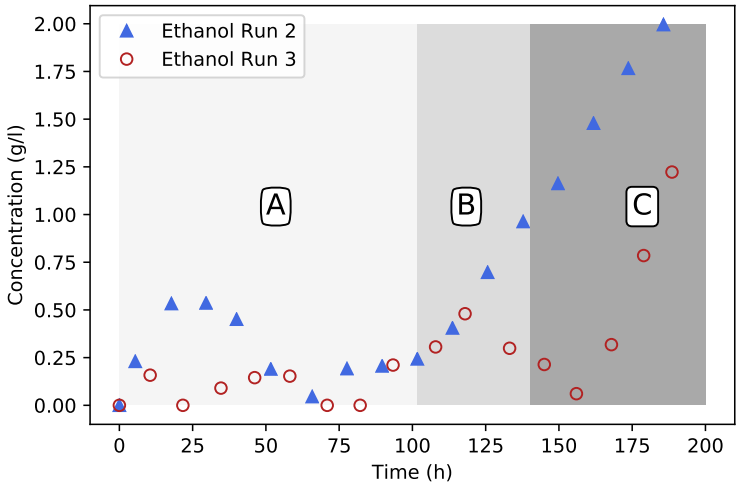

Figure 19: Ethanol profiles for run 2 and 3. No ethanol is produced in the first 25 h in run 3, as was the case in run 1 and 2 and could be expected.

In Figure 19 section A it can be seen that the initial production of ethanol, which was seen in both runs 1 and 2, is not present in run 3. Previously, the initial ethanol production was attributed to a transition phase from growth metabolism to production metabolism. If this is, in fact, the cause of ethanol production, then the response seen in run 3 suggests that the increased urea fed allowed for a faster transition, negating the initial ethanol production. Section B shows that there is an initial ethanol production after the second glucose feed step. The metabolism then soon shifts from ethanol production to ethanol consumption, which may be the result of the greater ability of *R. oryzae* to adapt, due to the higher nitrogen feed. This shows that ethanol overflow does not occur in section B, thus the overflow threshold is higher than in run 2. The greater availability of nitrogen may have allowed for the required protein synthesis, enabling more carbon to be directed to fumarate and respiration. Section C shows that the ethanol overflow point has been surpassed. This is at a glucose feed rate higher than that previously found, suggesting that there is an interplay between the overflow point and the carbon:nitrogen ratio. Further investigation will have to be conducted into the exact nitrogen content in the medium at the times of these responses to come to a definite conclusion about the mechanism of the effect.

The glucose concentration profile of run 3 (see Figure 20) can be seen to have a different profile from that of run 2. Section A shows that in both runs the glucose fed was fully consumed, but then in section B, when glucose accumulates in run 2, that is not seen in run 3. This suggests that during this period there is a higher glucose uptake rate in run 3, but the higher glucose uptake is not evident from the fumarate or ethanol production. In section C the glucose concentration begins to rise, indicating that the

maximum glucose uptake rate may have been surpassed. Since the fermentation ended while the concentration was rising, a stable glucose concentration was never reached. If a stable concentration had been reached it would have meant that the threshold uptake rate had not been surpassed. This would have enabled the calculation of the ethanol breakthrough point for this specific nitrogen feed rate. Since it seems that the ethanol breakthrough point and the threshold glucose uptake rate were surpassed in the same step they cannot be separated or calculated.

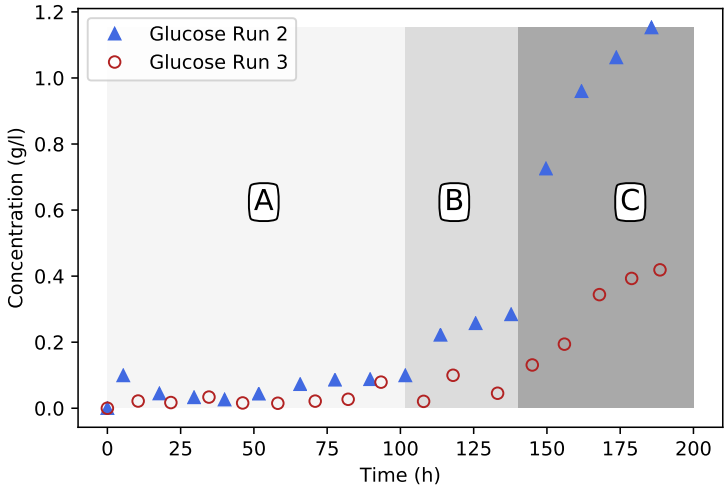

Figure 20: Glucose profiles for run 2 and 3. Glucose breakthrough observed for run 2 in regime C, where glucose addition rates exceeds glucose consumption rate.

Run 3 also experienced a considerable increase in biomass from the growth phase to the production phase. The biomass concentration of run 3 was found to be $3.27\,\mathrm{g\,L^{-1}}$, which is approximately a 30 % higher biomass concentration than in runs 1 and 2. A likely cause of this increased biomass concentration is the doubled nitrogen feed rate. The increased nitrogen availability allowed for further protein synthesis, which may also be a contributing factor to the observed results. Based on the amount of nitrogen fed to the system, the predicted biomass formation was only 8 %, which is far lower than the five-fold increase observed. As stated before, it is not believed that the biomass produced during the production phase was of equal metabolic activity to that produced during the growth phase. An investigation into the metabolic activity of this biomass will have to be conducted to fully understand this mechanism and determine the cause of the observed responses. The final yield was found to be $0.588\,\mathrm{g\,g^{-1}}$, which is similar to that of run 1. Run 3 produced less ethanol than run 1, and therefore it can be seen that the increased urea fed resulted in less ethanol production.

5 Conclusion

The production of fumarate using *Rhizopus oryzae* has always been associated with the simultaneous production of ethanol. It was hypothesised that the production of ethanol was a result of the Crabtree effect, a common overflow mechanism in yeasts. The production of ethanol was previously attributed to anaerobic zones within the mycelium matrix. Experiments with a five-fold increase in the dissolved oxygen content resulted in similar ethanol responses, suggesting that ethanol formation occurs under fully aerobic conditions within the fungal matrix.

Ethanol production by *S. cerevisiae* has been successfully negated using closely controlled glucose addition (Habegger *et al*, 2018). This method was employed in a biomass growth experiment with *Rhizopus oryzae*. It was found that a glucose feed rate of $0.07\,\mathrm{g\,L^{-1}\,h^{-1}}$ resulted in no ethanol production. These results indicated that *R. oryzae* is a Crabtree-positive organism since ethanol production was negated by manipulating the glucose feed rate.

Biomass production was not, however, the focus of this study. Therefore the same fed-batch strategy was tested for the nitrogen-limited fumarate production phase. A glucose feed rate was found that produced no ethanol while still producing fumarate. The ethanol overflow point was estimated to occur at a glucose feed rate of $0.395\,\mathrm{g\,g^{-1}\,h^{-1}}$, while the glucose breakthrough uptake rate lies between $0.426\,\mathrm{g\,g^{-1}\,h^{-1}}$ and $0.533\,\mathrm{g\,g^{-1}\,h^{-1}}$.

Additional parameters have been identified as promising avenues for optimising fumarate production. The first of these parameters tested was an increased nitrogen feed rate which resulted in decreased ethanol production while the fumarate yield was maintained. The remaining parameters will be the focus of further studies in the future.

The findings of this study conclusively prove that fumarate can be produced without the co-production of ethanol. The term homofumarate production" is used to describe the condition where all carbon exits the cell as either fumarate or respiratory CO_2. The result provides new insights toward developing a high-yielding industrial process to produce fumaric acid with *Rhizopus oryzae*.

References

Abe, A, Oda, Y, Asano, K and Sone, T (2007) "Rhizopus delemar is the proper name for *Rhizopus oryzae* fumaric-malic acid producers" *Mycologia*, *99*, (5): 714–722 ISSN: 00275514 DOI: 10.3852/mycologia.99.5.714.

Aiba, S, Nagai, S and Nishi, Y (1976) "A Perspective of Computer Control to Enhance the Productivity in Baker 's Yeast Cultivation" *Biotechnology*, *XVIII*, 1001–1016.

Barford, JP and Hall, RJ (1979) "An Examination of the Crabtree Effect in Saccharomyces cerevisiae: the Role of Respiratory Adaptation" *Journal of General Microbiology*, *114*, (2): 267–275 ISSN: 0022-1287 DOI: 10.1099/00221287-114-2-267 URL: http://mic.microbiologyresearch.org/content/journal/micro/10.1099/00221287-114-2-267%20https://www.microbiologyresearch.org/content/journal/micro/10.1099/00221287-114-2-267.

Bozell, JJ and Petersen, GR (2010) "Technology development for the production of biobased products from biorefinery carbohydrates-the US Department of Energy's "Top 10" revisited" *Green Chemistry*, *12*, (4): 539 ISSN: 1463-9262 DOI: 10.1039/b922014c URL: http://xlink.rsc.org/?DOI=b922014c.

Cao, N, Du, J, Chen, C, Gong, CS and Tsao, GT (1997) "Production of fumaric acid by immobilized *Rhizopus* using rotary biofilm contactor" *Applied Biochemistry and Biotechnology*, *63-65*, (1): 387–394 ISSN: 0273-2289 DOI: 10.1007/BF02920440 URL: http://link.springer.com/10.1007/BF02920440.

Committee of Experts on Cosmetic Products (2008) *Safety survey of active ingredients used in cosmetics*, Council of Europe, Strasbourg Cedex: pp. 159–160 ISBN: 978-92-871-6298-4 URL: http://book.coe.int.

Das, RK and Brar, SK (2014) "Enhanced Fumaric Acid Production from Brewery Wastewater and Insight into the Morphology of *Rhizopus oryzae* 1526" *Applied Biochemistry and Biotechnology*, *172*, (6): 2974–2988 ISSN: 0273-2289 DOI: 10.1007/s12010-014-0739-z URL: http://link.springer.com/10.1007/s12010-014-0739-z.

Das, RK, Brar, SK and Verma, M (2016) "Fumaric Acid" *Platform Chemical Biorefinery*, (June 2016): 133–157 DOI: 10.1016/b978-0-12-802980-0.00008-0.

Das, RK, Brar, SK and Verma, M (2015a) "A fermentative approach towards optimizing directed biosynthesis of fumaric acid by *Rhizopus oryzae* 1526 utilizing apple industry waste biomass" *Fungal Biology*, *119*, (12): 1279–1290 ISSN: 18786146 DOI: 10.1016/j.funbio.2015.10.001 URL: https://linkinghub.elsevier.com/retrieve/pii/S1878614615001907.

Das, RK, Brar, SK and Verma, M (2015b) "Enhanced fumaric acid production from brewery wastewater by immobilization technique" *Journal of Chemical Technology & Biotechnology*, *90*, (8): 1473–1479 ISSN: 02682575 DOI: 10.1002/jctb.4455 URL: http://doi.wiley.com/10.1002/jctb.4455.

Deng, Y, Li, S, Xu, Q, Gao, M and Huang, H (2012) "Production of fumaric acid by simultaneous saccharification and fermentation of starchy materials with 2-deoxyglucose-resistant mutant strains of *Rhizopus oryzae*" *Bioresource Technology*, *107*, 363–367 ISSN: 09608524 DOI: 10.1016/j.biortech.2011.11.117 URL: http://dx.doi.org/10.1016/j.biortech.2011.11.117.

Felthouse, TR, Burnett, JC, Horrell, B, Mummey, MJ and Kuo, YJ (2001) "Maleic Anhydride, Maleic Acid, and Fumaric Acid", in: *Kirk-Othmer Encyclopedia of Chemical Technology*, Felthouse, TR (Ed.), 10 John Wiley & Sons, Inc., Hoboken, NJ, USA DOI: 10.1002/0471238961.1301120506051220.a01.pub2 URL: http://doi.wiley.com/10.1002/0471740039.vec1569.

Fogler, HS (2006) *Elements of Chenzicn 1 Reaction Engineering*, ISBN: 0130473944.

Foster, JW and Waksman, SA (1939) "The Production of Fumaric Acid by Molds Belonging to the Genus Rhizopus" *Journal of the American Chemical Society*, *61*, (1): 127–135 ISSN: 15205126 DOI: 10.1021/ja01870a043.

Fu, YQ, Li, S, Chen, Y, Xu, Q, Huang, H and Sheng, XY (2010) "Enhancement of fumaric acid production by *Rhizopus oryzae* using a two-stage dissolved oxygen control strategy" *Applied Biochemistry and Biotechnology*, *162*, (4): 1031–1038 ISSN: 02732289 DOI: 10.1007/s12010-009-8831-5.

Giorno, L, Drioli, E, Carvoli, G, Cassano, A and Donato, L (2001) "Study of an enzyme membrane reactor with immobilized fumarase for production of L-malic acid" *Biotechnology & Bioengineering*, *72*, (1): 77–84 ISSN: 00063592 DOI: 10.1002/1097-0290(20010105)72:1<77::aid-bit11>3.3.co;2-c.

Grand View Research (2014) *Maleic Anhydride Market Analysis By Application(Unsaturated Polyster Resins, BDO, Additives, Copolymers) and SegmentForecasts To 2020* tech. rep.

Grand View Research (2019) *Fumaric Acid Market Size, Share & Trends Analysis Report By Application (Food & Beverages, Rosin Paper Sizes, Unsaturated Polyester Resins, Alkyd Resins), By Region, And Segment Forecasts, 2015 - 2022* URL: https://www.grandviewresearch.com/industry-analysis/fumaric-acid-market.

Gu, C, Zhou, Y, Liu, L, Tan, T and Deng, L (2013) "Production of fumaric acid by immobilized *Rhizopus arrhizus* on net" *Bioresource Technology*, *131*, 303–307 ISSN: 09608524 DOI: 10.1016/j.biortech.2012.12.148 URL: https://linkinghub.elsevier.com/retrieve/pii/S0960852412020068.

Habegger, L, Crespo, KR and Dabros, M (2018) "Preventing overflow metabolism in crabtree-positive microorganisms through on-line monitoring and control of fed-batch fermentations" *Fermentation*, *4*, (3) ISSN: 23115637 DOI: 10.3390/fermentation4030079.

Huang, L, Wei, P, Zang, R and Xu, Z (2010) "High-throughput screening of high-yield colonies of *Rhizopus oryzae* for enhanced production of fumaric acid": 287–292 DOI: 10.1007/s13213-010-0039-y.

Ilica, RA, Kloetzer, L, Galaction, AI and Caşcaval, D (2019) "Fumaric acid: production and separation" *Biotechnology Letters*, *41*, (1): 47–57 ISSN: 15736776 DOI: 10.1007/s10529-018-2628-y.

Jansen, ML and Gulik, WM van (2014) "Towards large scale fermentative production of succinic acid" *Current Opinion in Biotechnology*, *30*, 190–197 ISSN: 18790429 DOI: 10.1016/j.copbio.2014.07.003 URL: http://dx.doi.org/10.1016/j.copbio.2014.07.003.

Kang, SW, Lee, H, Kim, D, Lee, D, Kim, S, Chun, GT, Lee, J, Kim, SW and Park, C (2010) "Strain development and medium optimization for fumaric acid production" *Biotechnology and Bioprocess Engineering*, *15*, (5): 761–769 ISSN: 12268372 DOI: 10.1007/s12257-010-0081-4.

Lassey, KR (2008) "Livestock methane emission and its perspective in the global methane cycle" (Lassey 2007): 114–118.

Li, Z, Liu, N, Cao, Y, Jin, C, Li, F, Cai, C and Yao, J (2018) "Effects of fumaric acid supplementation on methane production and rumen fermentation in goats fed diets varying in forage and concentrate particle size" *Journal of Animal Science and Biotechnology*, *9*, (1): 1–9 ISSN: 20491891 DOI: 10.1186/s40104-018-0235-3.

Liao, W, Liu, Y, Frear, C and Chen, S (2007) "A new approach of pellet formation of a filamentous fungus - *Rhizopus oryzae*" *Bioresource Technology*, *98*, (18): 3415–3423 ISSN: 09608524 DOI: 10.1016/j.biortech.2006.10.028.

Liao, W, Liu, Y, Frear, C and Chen, S (2008) "Co-production of fumaric acid and chitin from a nitrogen-rich lignocellulosic material - dairy manure - using a pelletized filamentous fungus *Rhizopus oryzae* ATCC 20344" *Bioresource Technology*, *99*, (13): 5859–5866 ISSN: 09608524 DOI: 10.1016/j.biortech.2007.10.006 URL: https://linkinghub.elsevier.com/retrieve/pii/S0960852407008437.

Liu, H, Wang, W, Deng, L, Wang, F and Tan, T (2015) "High production of fumaric acid from xylose by newly selected strain Rhizopus arrhizus RH 7-13-9#" *Bioresource Technology*, *186*, 348–350 ISSN: 09608524 DOI: 10.1016/j.biortech.2015.03.109 URL: https://linkinghub.elsevier.com/retrieve/pii/S0960852415004411.

Liu, H, Zhao, S, Jin, Y, Yue, X, Deng, L, Wang, F and Tan, T (2017) "Production of fumaric acid by immobilized *Rhizopus arrhizus* RH 7-13-9# on loofah fiber in a stirred-tank reactor" *Bioresource Technology*, *244*, 929–933 ISSN: 09608524 DOI: 10.1016/j.biortech.2017.07.185 URL: https://linkinghub.elsevier.com/retrieve/pii/S0960852417313019.

Madigan, MT, Martinko, JM, Bender, KS, Buckley, DH, Stahl, DA and Brock, T (2015) *Brock biology of microorganisms*, 14th ed. Pearson: pp. 86–94 ISBN: 978-0-321-89739-8.

Martin-Dominguez, V, Estevez, J, Ojembarrena, F, Santos, V and Ladero, M (2018) "Fumaric Acid Production: A Biorefinery Perspective" *Fermentation*, *4*, (2): 33 DOI: 10.3390/fermentation4020033.

Moharregh-Khiabani, D, Linker, R, Gold, R and Stangel, M (2009) "Fumaric Acid and its Esters: An Emerging Treatment for Multiple Sclerosis" *Current Neuropharmacology*, *7*, (1): 60–64 ISSN: 1570159X DOI: 10.2174/157015909787602788.

Naude, A and Nicol, W (2017) "Fumaric acid fermentation with immobilised *Rhizopus oryzae*: Quantifying time-dependent variations in catabolic flux" *Process Biochemistry*,

56, 8–20 ISSN: 13595113 DOI: 10.1016/j.procbio.2017.02.027 URL: http://dx.doi.org/10.1016/j.procbio.2017.02.027.

Naude, A and Nicol, W (2018) "Improved continuous fumaric acid production with immobilised *Rhizopus oryzae* by implementation of a revised nitrogen control strategy" *New Biotechnology*, *44*, (July 2017): 13–22 ISSN: 18764347 DOI: 10.1016/j.nbt.2018.02.012 URL: https://doi.org/10.1016/j.nbt.2018.02.012.

Nystrom, RF, Loo, YH and Leak, JC (1952) "Synthesis of Fumaric Acid-2-C 14 and Maleic Anhydride-2-C 14 1" *Journal of the American Chemical Society*, *74*, (13): 3434–3435 ISSN: 0002-7863 DOI: 10.1021/ja01133a521 URL: http://pubs.acs.org/doi/abs/10.1021/ja01133a521.

Odoni, DI, Tamayo-Ramos, JA, Sloothaak, J, Heck, RG van, Martins dos Santos, VA, Graaff, LH de, Suarez-Diez, M and Schaap, PJ (2017) "Comparative proteomics of Rhizopus delemar ATCC 20344 unravels the role of amino acid catabolism in fumarate accumulation" *PeerJ*, *5*, e3133 ISSN: 2167-8359 DOI: 10.7717/peerj.3133 URL: https://peerj.com/articles/3133.

Papadaki, A, Androutsopoulos, N, Patsalou, M, Koutinas, M, Kopsahelis, N, Castro, A, Papanikolaou, S and Koutinas, A (2017) "Biotechnological Production of Fumaric Acid: The Effect of Morphology of Rhizopus arrhizus NRRL 2582" *Fermentation*, *3*, (3): 33 DOI: 10.3390/fermentation3030033.

Peleg, Y, Battat, E, Scrutton, MC and Goldberg, I (1989) "Isoenzyme pattern and subcellular localisation of enzymes involved in fumaric acid accumulation by *Rhizopus oryzae*" *Applied Microbiology and Biotechnology*, *32*, (3): 334–339 ISSN: 01757598 DOI: 10.1007/BF00184985.

Rhodes, RA, Lagoda, AA, Misenheimer, TJ, Smith, ML, Anderson, RF and Jackson, RW (1962) "Production of Fumaric Acid in 20-Liter Fermentors." *Applied microbiology*, *10*, (1): 9–15 ISSN: 0003-6919 URL: http://www.ncbi.nlm.nih.gov/pubmed/16349614%0Ahttp://www.pubmedcentral.nih.gov/articlerender.fcgi?artid=PMC1057800.

Roa Engel, CA, Gulik, WM van, Marang, L, Wielen, LA van der and Straathof, AJ (2011) "Development of a low pH fermentation strategy for fumaric acid production by *Rhizopus oryzae*" *Enzyme and Microbial Technology*, *48*, (1): 39–47 ISSN: 01410229 DOI: 10.1016/j.enzmictec.2010.09.001 URL: http://dx.doi.org/10.1016/j.enzmictec.2010.09.001%20https://linkinghub.elsevier.com/retrieve/pii/S0141022910001948.

Roa Engel, CA, Straathof, AJJ, Zijlmans, TW, Van Gulik, WM and Van Der Wielen, LAM (2008) "Fumaric acid production by fermentation" *Applied Microbiology and Biotechnology*, *78*, (3): 379–389 ISSN: 01757598 DOI: 10.1007/s00253-007-1341-x.

Sebastian, J, Hegde, K, Kumar, P, Rouissi, T and Brar, SK (2019) "Bioproduction of fumaric acid: an insight into microbial strain improvement strategies" *Critical Reviews in Biotechnology*, *39*, (6): 817–834 ISSN: 15497801 DOI: 10.1080/07388551.2019.1620677 URL: https://doi.org/10.1080/07388551.2019.1620677.

Song, CW, Kim, DI, Choi, S, Jang, JW and Lee, SY (2013) "Metabolic engineering of Escherichia coli for the production of fumaric acid" *Biotechnology and Bioengineering*, *110*, (7): 2025–2034 ISSN: 00063592 DOI: 10.1002/bit.24868 URL: https://onlinelibrary.wiley.com/doi/abs/10.1002/bit.24868.

Stojkovič, G and Žnidaršič-Plazl, P (2012) "Continuous synthesis of l-malic acid using whole-cell microreactor" *Process Biochemistry*, *47*, (7): 1102–1107 ISSN: 13595113 DOI: 10.1016/j.procbio.2012.03.023 URL: https://linkinghub.elsevier.com/retrieve/pii/S1359511312001377.

Suijdam, JC van, Kossen, NW and Paul, PG (1980) "An inoculum technique for the production of fungal pellets" *European Journal of Applied Microbiology and Biotechnology*, *10*, (3): 211–221 ISSN: 01711741 DOI: 10.1007/BF00508608.

Taymaz-Nikerel, H, Jamalzadeh, E, Borujeni, AE, Verheijen, PJ, Van Gulik, WM and Heijnen, SJ (2013) "A thermodynamic analysis of dicarboxylic acid production in microorganisms" *Biothermodynamics: The Role of Thermodynamics in Biochemical Engineering*, 547–579.

The Oxford Encyclopedia of Food and Drink in America, (2012) Oxford University Press ISBN: 9780199734962 DOI: 10.1093/acref/9780199734962.001.0001 URL: http://www.oxfordreference.com/view/10.1093/acref/9780199734962.001.0001/acref-9780199734962.

Verduyn, C, Zomerdijk, TPL, Dijken, JP van and Scheffers, WA (1984) "Continuous measurement of ethanol production by aerobic yeast suspensions with an enzyme electrode" *Applied Microbiology and Biotechnology*, *19*, (3): 181–185 ISSN: 01757598 DOI: 10.1007/BF00256451.

Villadsen, J, Nielsen, J and Lidén, G (2011) *Bioreaction Engineering Principles*, Springer US, Boston, MA ISBN: 978-1-4419-9687-9 DOI: 10.1007/978-1-4419-9688-6 URL: http://link.springer.com/10.1007/978-1-4419-9688-6.

Wang, G, Huang, D, Qi, H, Wen, J, Jia, X and Chen, Y (2013) "Rational medium optimization based on comparative metabolic profiling analysis to improve fumaric acid production" *Bioresource Technology*, *137*, 1–8 ISSN: 18732976 DOI: 10.1016/j.biortech.2013.03.041 URL: http://dx.doi.org/10.1016/j.biortech.2013.03.041.

Warren, R, Barker, J, Van de Kerkhof, P, Reich, K and Mrowietz, U (2019) "Switching from a fumaric acid ester mixture to dimethylfumarate monotherapy in psoriasis" *Journal of the European Academy of Dermatology and Venereology*, *33*, (10): 0–2 ISSN: 0926-9959 DOI: 10.1111/jdv.15644 URL: https://onlinelibrary.wiley.com/doi/abs/10.1111/jdv.15644.

Wen, S, Liu, L, Nie, K, Deng, L, Tan, T and Wang, F (2013) "Enhanced Fumaric Acid Production by Fermentation of Xylose Using a Modified Strain of Rhizopus arrhizus" *Bioresources*, *8*, DOI: 10.15376/biores.8.2.2186-2194.

Werpy, T and Petersen, GR (2004) *Top Value Added Chemicals from Biomass: Volume I – Results of Screening for Potential Candidates from Sugars and Synthesis Gas* tech. rep. Golden, CO (United States): National Renewable Energy Laboratory (NREL): p. 76 DOI: 10.2172/15008859 URL: http://www.osti.gov/scitech//servlets/purl/15008859-s6ri0N/native/%20http://www.osti.gov/servlets/purl/15008859/.

Wojcieszak, R, Santarelli, F, Paul, S, Dumeignil, F, Cavani, F and Gonçalves, RV (2015) "Recent developments in maleic acid synthesis from bio-based chemicals" *Sustainable Chemical Processes*, *3*, (1): 1–11 ISSN: 2043-7129 DOI: 10.1186/s40508-015-0034-5.

Xu, G, Chen, X, Liu, L and Jiang, L (2013) "Fumaric acid production in Saccharomyces cerevisiae by simultaneous use of oxidative and reductive routes" *Bioresource Technology*, *148*, 91–96 ISSN: 18732976 DOI: 10.1016/j.biortech.2013.08.115 URL: http://dx.doi.org/10.1016/j.biortech.2013.08.115.

Xu, Q, Li, S, Fu, Y, Tai, C and Huang, H (2010) "Two-stage utilization of corn straw by *Rhizopus oryzae* for fumaric acid production" *Bioresource Technology*, *101*, (15): 6262–6264 ISSN: 09608524 DOI: 10.1016/j.biortech.2010.02.086 URL: https://linkinghub.elsevier.com/retrieve/pii/S0960852410003974.

Xu, Q, Li, S, Huang, H and Wen, J (2012) "Key technologies for the industrial production of fumaric acid by fermentation" *Biotechnology Advances*, *30*, (6): 1685–1696 ISSN: 07349750 DOI: 10.1016/j.biotechadv.2012.08.007 URL: http://dx.doi.org/10.1016/j.biotechadv.2012.08.007.

Zhang, B, Skory, CD and Yang, ST (2012) "Metabolic engineering of *Rhizopus oryzae*: Effects of overexpressing pyc and pepc genes on fumaric acid biosynthesis from glucose" *Metabolic Engineering*, *14*, (5): 512–520 ISSN: 10967176 DOI: 10.1016/j.ymben.2012.07.001 URL: https://linkinghub.elsevier.com/retrieve/pii/S1096717612000717.

Zhang, K, Yu, C and Yang, ST (2015) "Effects of soybean meal hydrolysate as the nitrogen source on seed culture morphology and fumaric acid production by *Rhizopus oryzae*" *Process Biochemistry*, *50*, (2): 173–179 ISSN: 13595113 DOI: 10.1016/j.procbio.2014.12.015 URL: http://dx.doi.org/10.1016/j.procbio.2014.12.015.

Zhang, K, Zhang, B and Yang, ST (2013) "Production of Citric, Itaconic, Fumaric, and Malic Acids in Filamentous Fungal Fermentations" *Bioprocessing Technologies in Biorefinery for Sustainable Production of Fuels, Chemicals, and Polymers*, (July 2013): 375–398 DOI: 10.1002/9781118642047.ch20.

Zhou, Y, Du, J and Tsao, GT (2000) "Mycelial Pellet Formation by *Rhizopus oryzae* ATCC 20344" *Applied Biochemistry and Biotechnology*, *84-86*, (1-9): 779–790 ISSN: 0273-2289 DOI: 10.1385/ABAB:84-86:1-9:779 URL: http://link.springer.com/10.1385/ABAB:84-86:1-9:779.

Zhou, Y, Nie, K, Zhang, X, Liu, S, Wang, M, Deng, L, Wang, F and Tan, T (2014) "Production of fumaric acid from biodiesel-derived crude glycerol by Rhizopus arrhizus" *Bioresource Technology*, *163*, 48–53 ISSN: 09608524 DOI: 10.1016/j.biortech.2014.04.021 URL: https://linkinghub.elsevier.com/retrieve/pii/S0960852414005161.

Zhou, Z, Du, G, Hua, Z, Zhou, J and Chen, J (2011) "Optimization of fumaric acid production by Rhizopus delemar based on the morphology formation" *Bioresource Technology*, *102*, (20): 9345–9349 ISSN: 09608524 DOI: 10.1016/j.biortech.2011.07.120 URL: http://dx.doi.org/10.1016/j.biortech.2011.07.120.